

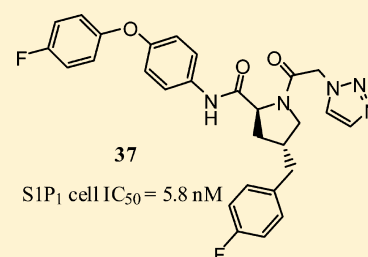
Discovery of a Novel Class of Potent and Orally Bioavailable Sphingosine 1-Phosphate Receptor 1 Antagonists

Mohamed A. Ibrahim, Henry W. B. Johnson,* Joon Won Jeong, Gary L. Lewis, Xian Shi, Robin T. Noguchi, Matthew Williams, James W. Leahy, John M. Nuss, John Woolfrey, Monica Banica, Frauke Bentzien, Yu-Chien Chou, Anna Gibson, Nathan Heald, Peter Lamb, Larry Mattheakis, David Matthews, Aaron Shipway, Xiang Wu, WenTao Zhang, Sihong Zhou, and Geetha Shankar

Department of Drug Discovery, Exelixis, 169 Harbor Way, South San Francisco, California 94083, United States

S Supporting Information

ABSTRACT: A series of subtype selective sphingosine 1-phosphate receptor 1 (S1P₁) antagonists are disclosed. Our high-throughput screening campaign revealed hit **1** for which an increase in potency and mouse oral exposure was achieved with minor modifications to the chemical scaffold. In vivo efficacy revealed that at high doses compounds **12** and **15** inhibited tumor growth. Further optimization of our lead series led to the discovery of proline derivatives **37** (XL541) and **38** which had similar efficacy as our first generation analogues at significantly lower doses. Analogue **37** displayed excellent pharmacokinetics and oral exposure in multiple species.



INTRODUCTION

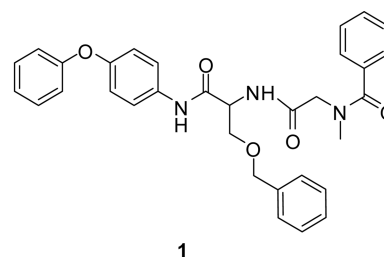
Sphingosine 1-phosphate (S1P) is a bioactive lipid that has demonstrated effects on a variety of different cellular processes including cell growth, apoptosis, cytoskeletal rearrangement, cell motility, angiogenesis, and vascular maturation.^{1–6} Of the five known S1P receptors, sphingosine 1-phosphate receptor 1 (S1P₁) was the first receptor discovered, and 8 years later it was orphanized when S1P was disclosed as the natural ligand.^{6,7}

In 2000, a groundbreaking demonstration of the role S1P₁ plays during vascular maturation in developing embryos was disclosed.⁸ Global deletion of S1P₁ causes embryonic death in mice as a result of excessive intraembryonic hemorrhaging. Interestingly, the developing mice exhibit normal vasculogenesis and angiogenesis but suffer severe impairment in vessel maturation. In addition, the role of S1P₁ in immune regulation was serendipitously unmasked by the clinical benefit seen with the agonist 2-amino-2-(4-octylphenethyl)propane-1,3-diol (fingolimod, FTY720) which causes sequestration of lymphocytes into secondary lymphoid organs and blocks the egress of mature thymocytes from the thymus.⁹ In 2010, fingolimod was approved as the first oral medication for the treatment of multiple sclerosis.

Various reports describing the activity and pharmacology of selective small molecule S1P₁ agonists exist.^{10,11} However, fewer efforts to target S1P₁ with selective antagonists have been disclosed.^{12–14} Knowing that S1P₂ has opposing signaling pathways to S1P₁ and that S1P₃ is implicated in causing undesired cardiac side effects,^{15,16} we aimed to develop a selective, orally bioavailable S1P₁ antagonist for use as a tool to explore the impact of S1P₁ antagonism on angiogenesis and tumor growth.

RESULTS AND DISCUSSION

An extensive screening campaign revealed the dipeptide derivative **1** having potent and, perhaps more important, selective antagonist activity vs S1P₁ (Figure 1). However, further



cAMP assay IC ₅₀	Luciferase Selectivity Assay IC ₅₀ (μM)			Mouse PO (1h and 4h at 100 mpk)
	S1P ₁	S1P ₂	S1P ₃	
718 nM	2.8	>10	>10	<0.019 μM

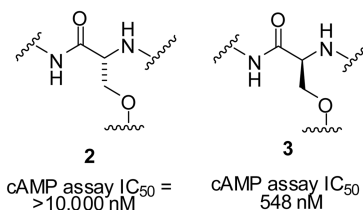


Figure 1. Structure and early data for racemic HTS hit compound **1** and optically pure analogues **2** and **3**.

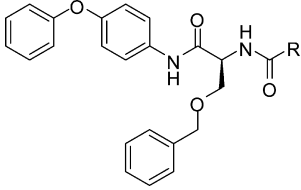
Received: November 14, 2011

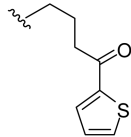

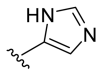
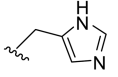
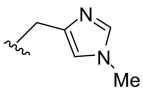
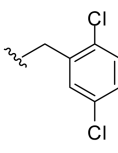
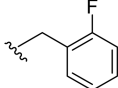
Published: January 3, 2012

evaluation of the pharmacokinetic profile of **1** demonstrated that no material was observed in the plasma above the limit of detection when dosed orally in mice after 1 and 4 h. It was also discovered that the *S*-enantiomer (**3**) gave rise to all the activity observed from the racemate, as it was >18-fold more potent than the *R*-enantiomer (**2**). At the outset, our goal was to improve the potency in our cAMP and luciferase selectivity assays, increase the oral exposure, and maintain a >10 μM potency threshold vs the S1P₂ and S1P₃ isoforms.

Initially, we wished to determine if the potency of **1** could be improved by changing functional groups on the periphery of the molecule. Data for analogues such as **4** and **5**, containing different sized R groups, indicated it was likely that further modification of this region would be tolerated (Table 1).

Table 1. Right-Hand Amide Analogues of HTS Lead 1



Compound	R	cAMP assay IC ₅₀ (nM)
4^a		286
5^a		297
6		> 1000
7		33
8		228
9		> 10000
10		500

^aRacemic material.

Particularly analogue **5**, containing a cyclopropanecarboxamide linkage, provided evidence that the *N*-methylbenzamide group of **1** could be removed, thereby lowering the molecular weight significantly while retaining modest potency. Comparison of

analogues with heterocyclic R groups, such as **6** and **7**, indicated that inserting a methylene spacer between the carboxyl group and heterocycle improved the potency >30-fold. In addition, **7** exhibited significantly higher mouse exposure than the HTS hit **1** when dosed at 100 mpk: 5 μM (1 h) and 3 μM (4 h) dosed as a solution in 10% EtOH/40% PEG400/water + 1:1 HCl, 100 mpk, or 4.4 μM (1 h) and 0.3 μM (4 h) dosed as a suspension in 10% NMP/corn oil. Improved mouse oral exposure was likely due in part to decreased mouse liver microsome (MLM) oxidation of **7** compared to HTS hit **1** (28% for **7** vs 89% conversion for **1** at 30 min). *N*-Substitution on the imidazole with a methyl group to afford **8** led to a loss in potency. In addition, compounds **9** and **10** demonstrated that hydrophobic aryl groups were less tolerated. In summary, optimizing the *N*-methylbenzamide group present in **1** allowed us to improve the potency approximately 1 log unit and significantly increase the mouse oral exposure.

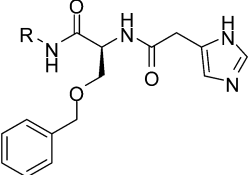
Analogues were next explored on the left-hand side, utilizing the optimized imidazole heterocycle as a standard (Table 2). As indicated by compounds **11–13** and **15**, placing electron withdrawing substituents around both aryl rings revealed that para-substitution of the phenyl ether was well tolerated. However, for reasons that are not entirely clear, inactive analogue **14** was an exception to this trend. Alkyl and benzyl substitutions generally resulted in a loss of potency (**16**, **17**). Also, interestingly, replacement of the phenoxy phenyl ether linkage with carbon or nitrogen and restricting rotation of this moiety significantly lowered activity (**18–21**) compared to parent **7**. Although modifications on the left-hand side of **1** did not result in as dramatic an improvement in potency as modifications on the right, analogue **15** demonstrated a ~2-fold improvement in potency. In addition, the MLM oxidation was lower in both the fluoro and chloro analogues **12** and **15** vs the parent **7** (9% conversion for **12** and **15** vs 28% conversion for **7** at 30 min). Lower MLM data not surprisingly translated to slightly improved mouse oral exposure for both **12** and **15** over the des-halogenated parent **7** (Table 3). The subtype selectivity was consistently monitored throughout the evolution of the program, and we were pleased to find that compounds **12** and **15** compared favorably to HTS hit **1** in that the S1P₁ activity was improved and a >10 μM potency threshold vs S1P₂ and S1P₃ was maintained.

Lastly, a series of amino acid analogues were explored to probe the SAR of the benzyl ether group (Table 4). A comparison of **7** with **22** indicated that replacing the ether oxygen with carbon maintained activity. In addition, attempts to truncate the alkyl chain revealed a loss in potency as indicated by **23** and **24**.

Since analogues **12** and **15** demonstrated good potency and moderate oral bioavailability, we decided to probe the anti-cancer efficacy of these agents. Specifically, compounds **12** and **15** were administered orally to animals implanted with MBA-MB-231T (breast adenocarcinoma) xenografts to determine their effect on tumor growth. We decided to additionally compare our compounds to both the VEGFR2/EGFR antagonist **25** and Merck S1P1 receptor agonist **26**.^{17,18} Tumor growth was measured over time starting on day 14 after implantation (Figure 2). Data were collected five times over 14 days. Dosing compounds **12** and **15** at 300 mpk resulted in tumor growth inhibition of 45% and 54%, respectively, data which were comparable to a lower dosage of both **25** and **26**. In addition, in all five xenograft studies minimal weight loss was observed (see Supporting Information).

While it was encouraging that the initial proof-of-concept efficacy study was a success in that the compounds were well tolerated and able to modulate tumor growth, further optimization

Table 2. Serine 4-Phenoxyaniline Analogues



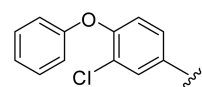
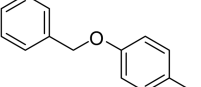
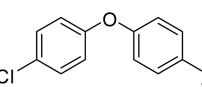
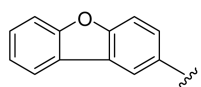
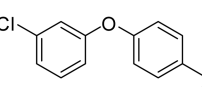
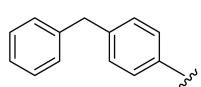
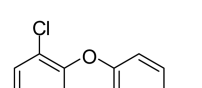
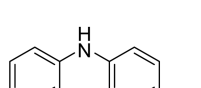
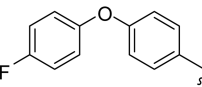
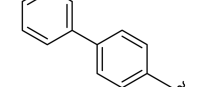
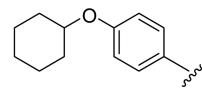
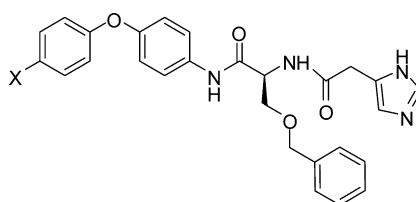
Compound	R	cAMP assay IC ₅₀ (nM)	Compound	R	cAMP assay IC ₅₀ (nM)
11		211	17		152
12		32	18		> 10000
13		96	19		> 10000
14		> 10000	20		743
15		13	21		> 10000
16		702			

Table 3. Summary of Data for Compounds 12 and 15



compound	X	cAMP assay IC ₅₀ (nM)	luciferase selectivity assay IC ₅₀ (nM)			mouse PO (100 mg/kg) (μM)	
			SIP ₁	SIP ₂	SIP ₃	1 h	4 h
12	Cl	32	221	>10000	>10000	11 ^a	11 ^a
15	F	13	284	>10000	>10000	8 ^b	3 ^b

^a10% EtOH/45% PEG400/water + 1:1 HCl. ^b10% EtOH/40% PEG400/water + 1:1 HCl.

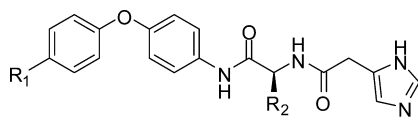
of this series was desired to produce analogues that could have greater effect at lower doses. In efforts to further improve upon compounds 12 and 15, modification of the serine core was next examined.

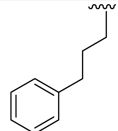
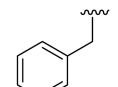
To this end, methylated amides of compound 7 were evaluated (Table 5). While the substituted alkylamide 27 led to a ~1 log unit decrease in activity, the aryl substituted amide 28 resulted in a more dramatic ~2.5 log unit loss of activity. Knowing that methylation of the arylamide was not tolerated with compound 28 and that reducing the number of rotatable

bonds often correlates inversely with oral bioavailability, a series of constrained analogues that left the donor/acceptor moiety of the arylamide intact were pursued.¹⁹ By utilization of this strategy, benzimidazole 29 and piperidine 30 were the first analogues synthesized (Table 6). While neither cyclic derivative improved the potency when compared to 15, it was encouraging that modifications of this kind were tolerated.

Considering the pharmacophoric features of earlier analogues and knowing that substitution of the alkylamide was tolerated, cyclization of the serine core to the proline derivative 31 was

Table 4. Benzyl Ether Modifications of Lead Series



Compound	R ₁	R ₂	cAMP assay IC ₅₀ (nM)
22	H		14
23	Cl	Me	752
24	Cl		326

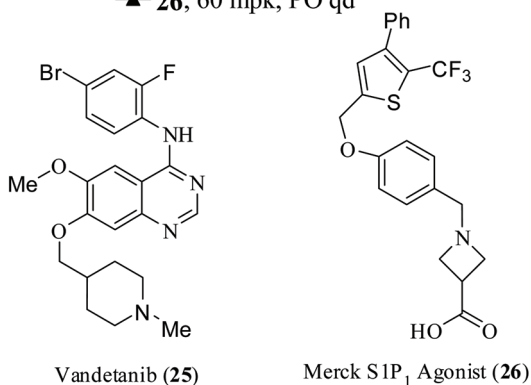
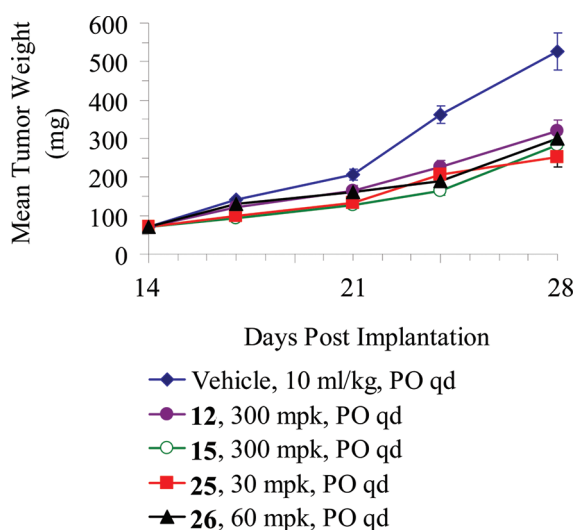
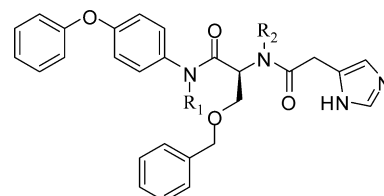


Figure 2. Effect of treatment with compounds 12 and 15 on MDA-MB-231T tumor volume. Tumor weight is an average of 10 animals per group on day of the indicated treatment. Dosing period was days 14–28.

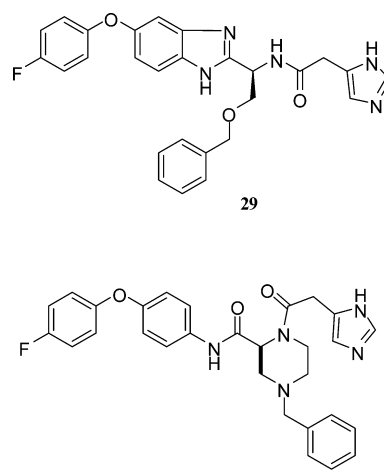
pursued. While 31 was ~6-fold less potent than 15, we were encouraged that the mouse exposure of this analogue was slightly higher than those of earlier analogues at the 1 h time point (Table 7). The increase in exposure appeared to be general in that phenyl derivative 32 demonstrated mouse

Table 5. Serine Amide Methyl Substitutions



compound	R ₁	R ₂	cAMP assay IC ₅₀ (nM)
27	H	Me	181
28	Me	H	8281

Table 6. Data for Cyclized Analogues 29 and 30



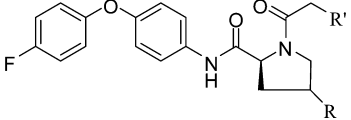
compound	cAMP assay IC ₅₀ (nM)	mouse PO (100 mg/kg)
29	239	18.7 μM ^a (1 h) 2.7 μM ^a (4 h)
30	84	6.3 μM ^b (4 h) 9.2 μM ^b (24 h)

^a10% EtOH/40% PEG400/20% Captisol/water + 1:1 HCl. ^b10% NMP/corn oil.

exposure levels at 4 and 24 h comparable to levels of other analogues at the earlier 1 and 4 h time points.

In efforts to reduce the CYP 3A4 liability of analogues 31 and 32, triazoles 33 and 34 were synthesized. While triazole analogue 33 was less active than the parent 32, we were pleased to find that triazole 34 simultaneously optimized CYP 3A4 inhibition, improved the potency ~1 log unit, and incrementally improved the mouse exposure when compared to the parent 31. Fluoro-substituted analogue 35 was synthesized to improve the MLM oxidation of 34 (13% conversion at 30 min in 34 vs 8% conversion in 35), which in turn provided greater mouse oral exposure as well. To determine if the stereochemistry at C-4 was optimal, we synthesized the cis isomer 36, which was ~1 log unit less active than the parent trans analogue 35. After modulation of the potency and mouse oral exposure to acceptable levels, the 2C9 and 2D6 CYP inhibition observed with 35 was addressed. Replacement of the 1,2,4-triazole 35 with the 1,2,3-triazole analogue 37 (XL541)²⁰ resulted in ~3-fold less 2D6 and ~8-fold less 2C9 activity. The 1,2,5-triazole 38 also had an optimized CYP inhibition profile. As we had anticipated based on data from the serine series, the enantiomer of 37 again provided evidence that the C-2 R-enantiomer was

Table 7. Data for Proline Series Analogues



Compound	R	R'	cAMP assay IC ₅₀ (nM)	Mouse PO (μM, 100 mg/kg) ^a	CYP inhibition IC ₅₀ (nM)			Luciferase Selectivity Assay IC ₅₀ (nM)
					2C9	2D6	3A4	
31			84.7	26.2 @ 1h, 9.8 @ 4h	< 205	1184	7146	-
32			158	27.2 @ 4h, 5.0 @ 24 h	213	663	301	-
33			492	-	-	-	-	-
34			6.8	86.4 @ 4h, 8.3 @ 24 h	2286	392	> 20000	45 (S1P ₁) > 10000 (S1P ₂) > 10000 (S1P ₃)
35			5.8	104 @ 4h, 18 @ 24 h	2187	7367	12605	13 (S1P ₁) > 10000 (S1P ₂) > 10000 (S1P ₃)
36			48	-	1347	3775	> 20000	-
37			5.8	16.7 @ 4h, 4.7 @ 24 h	17253	20325	> 20000	26 (S1P ₁) > 10000 (S1P ₂) > 10000 (S1P ₃)
ent-37			> 1000	-	-	-	-	-
38			4.8	23 @ 4h, 2.0 @ 24h	17390	> 50000	> 20000	21 (S1P ₁) > 10000 (S1P ₂) > 10000 (S1P ₃)

^a10% NMP/corn oil.

less potent than the *S*-enantiomer. Analogues **34**, **35**, **37**, and **38** were potent in the S1P₁ luciferase selectivity assay and demonstrated a >10 μM activity for S1P₂ and S1P₃.

To determine if the optimized proline series would translate to an improved profile in vivo, we again decided to test the efficacy of our compounds in the MDA-MB-231T mouse xenograft model. Compounds **37** and **38** were dosed for 14 days at 100 mpk, at which point we observed a statistically significant 43% and 60% tumor growth inhibition for **37** and **38**, respectively, data that were similar to those of earlier leads **12** and **15**, albeit at 1/3 of the dose (Figure 3).

On the basis of the excellent pharmacokinetic profile of **37** in the mouse and rat, it was chosen to be evaluated in higher order species (Table 8). The compound exhibits good oral exposure in rat, dog, and monkey when it is administered as a solution. Bioavailabilities of >40% were observed at 3 mpk along with long half-lives of >6 h. The oral exposure (AUC_{0-∞}) observed in the rat was 108 μM·h, and it was 108 μM·h in the dog and 16.7 μM·h in the monkey. Figure 4 shows the pharmacokinetic profile of **37** when dosed as a solution in cynomolgus monkey at 3 mpk.

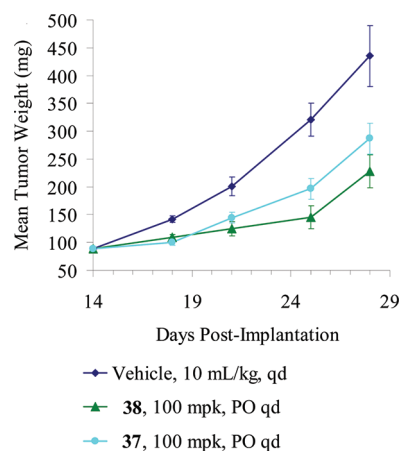


Figure 3. Effect of treatment with compounds **37** and **38** on MDA-MB-231T tumor volume. Tumor weight is an average of 10 animals per group on day of the indicated treatment. Dosing was days 14–28.

CHEMISTRY

Serine derivatives **1–10** and **27** could be synthesized as shown in Scheme 1. The appropriate protected benzylserine **39** or **40** was exposed to 4-phenoxyaniline using peptidic coupling

Table 8. Oral Pharmacokinetic Parameters for 37 in Rat, Dog, and Monkey (3 mpk, po)^a

parameter	rat	dog	monkey
C _{max} (μM)	3.2	5.4	1.5
t _{1/2} (h)	22.5	34.0	6.4
AUC _(0-∞) (μM·h)	107.5	107.9	16.7
F (%)	76.4	99.9	45.7

^aValues reported are the mean of three independent determinations. Compound was dosed as a solution in 5% EtOH/45% PEG400/water.

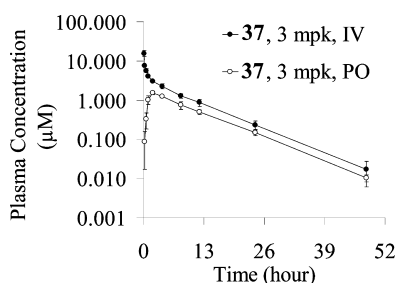
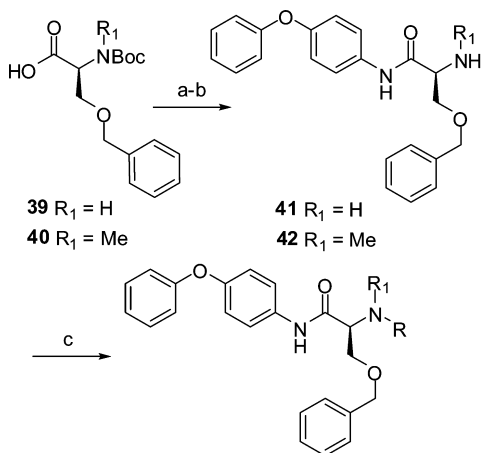


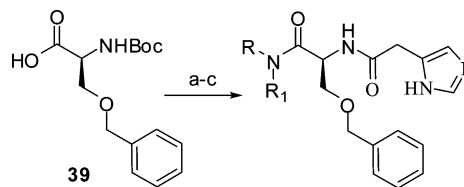
Figure 4. Pharmacokinetic profile of 37 in monkey. Compound 37 dosed at 3 mpk in male cynomolgus monkeys. The iv and po formulation was 5% EtOH/45% PEG400/water.

Scheme 1^a

Compound	RCOOH	R ₁
1 (rac)	2-(<i>N</i> -methylbenzamido)acetic acid	H
2 (ent)	2-(<i>N</i> -methylbenzamido)acetic acid	H
3	2-(<i>N</i> -methylbenzamido)acetic acid	H
4	5-oxo-5-(thiophen-2-yl)pentanoic acid	H
5	cyclopropanecarboxylic acid	H
6	1 <i>H</i> -imidazole-5-carboxylic acid	H
7	2-(1 <i>H</i> -imidazol-5-yl)acetic acid	H
8	2-(1-methyl-1 <i>H</i> -imidazol-4-yl)acetic acid	H
9	2-(2,5-dichlorophenyl)acetic acid	H
10	2-(2-fluorophenyl)acetic acid	H
27	2-(1 <i>H</i> -imidazol-5-yl)acetic acid	Me

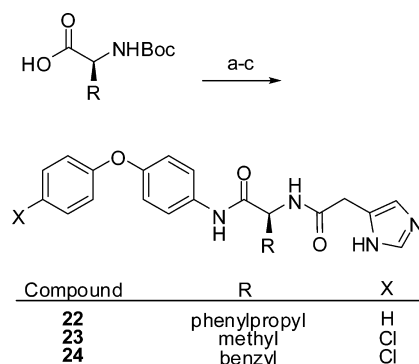
^aReagents: (a) HATU, DMF, *N,N*-diisopropylethylamine, 4-phenoxyaniline; (b) HCl (4 N in dioxane); (c) RCOOH, HATU, *N,N*-diisopropylethylamine, DMF.

conditions with *O*-(7-azabenzotriazol-1-yl)-*N,N,N',N'*-tetramethyluronium hexafluorophosphate (HATU), followed by Boc deprotection and diversification with a variety of acid coupling partners. The Boc derivatives 11–21 and 28 in Scheme 2 were synthesized using a similar methodology.

Scheme 2^a

R-NH ₂	R ₁
11: 3-chloro-4-phenoxyaniline	H
12: 4-(4-chlorophenoxy)aniline	H
13: 4-(3-chlorophenoxy)aniline	H
14: 4-(2-chlorophenoxy)aniline	H
15: 4-(4-fluorophenoxy)aniline	H
16: 4-(cyclohexyloxy)aniline	H
17: 4-(benzyloxy)aniline	H
18: dibenzo[<i>b,d</i>]furan-2-amine	H
19: 4-benzylaniline	H
20: <i>N</i> ¹ -phenylbenzene-1,4-diamine	H
21: biphenyl-4-amine	H
28: <i>N</i> -methyl-4-phenoxyaniline	Me

^aReagents: (a) HATU, DMF, *N,N*-diisopropylethylamine, R-NH₂; (b) HCl (4 N in dioxane); (c), HATU, *N,N*-diisopropylethylamine, DMF, 2-(1*H*-imidazol-5-yl)acetic acid.

Scheme 3^a

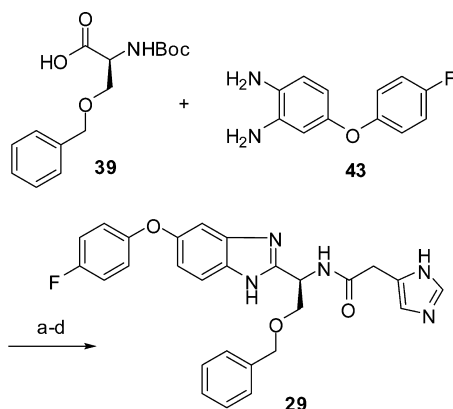
^aReagents: (a) HATU, DMF, *N,N*-diisopropylethylamine, 4-phenoxyaniline or 4-(4-chlorophenoxy)aniline; (b) HCl (4 N in dioxane); (c) HATU, *N,N*-diisopropylethylamine, DMF, 2-(1*H*-imidazol-5-yl)acetic acid.

Scheme 3 depicts the synthesis of different alkyl amino acids. Starting from the appropriate Boc-protected amino acid, the final compounds 22–24 were synthesized in a similar manner as described for Scheme 1.

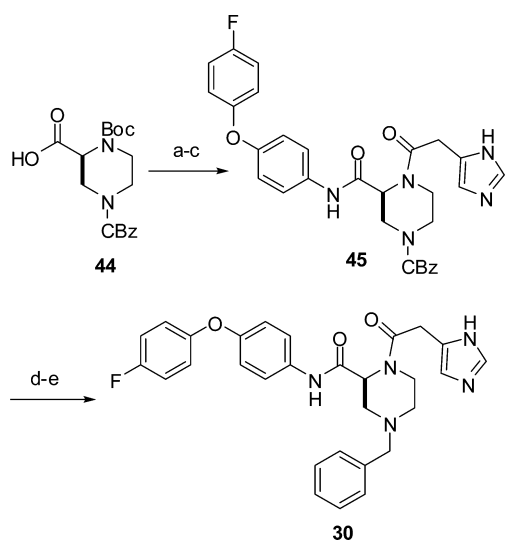
Scheme 4 depicts the synthesis of benzimidazole derivative 29. Coupling of 39 and 43 was carried out under peptidic coupling conditions followed by an acidic cyclization and coupling to 2-(1*H*-imidazol-5-yl)acetic acid to provide final compound 29.

The synthesis of derivative 30 originated from the diprotected commercially available piperazine 44 which was elaborated to provide 45 in a manner similar to previous methods in Scheme 1 (Scheme 5). Removing the benzyl carbamate (CBz) group followed by reductive amination provided 30.

The trans proline derivatives 31–35, 37, and 38 were synthesized as described in Scheme 6 in 10 steps starting from L-pyrogutamic acid 46. Diprotection followed by enolate formation and electrophile addition at low temperature provided alkylated derivatives 47–49. As expected, stereochemistry at the C-2 stereocenter was conserved during the alkylation step.²¹ Reduction of the lactam in two steps followed by ester hydrolysis, Boc protection, coupling with the appropriate phenoxyaniline,

Scheme 4^a

^aReagents: (a) HATU, *N,N*-diisopropylethylamine, DMF; (b) AcOH, 60 °C; (c) HCl (4 N in dioxane); (d) 4-imidazoleacetic acid hydrochloride, HATU, *N,N*-diisopropylethylamine, DMF.

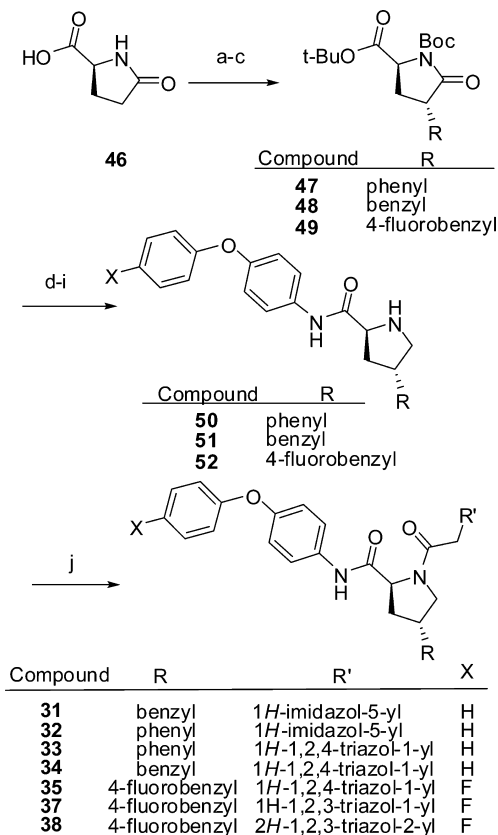
Scheme 5^a

^aReagents: (a) 4-(4-fluorophenoxy)aniline, HATU, *N,N*-diisopropylethylamine, DMF; (b) HCl (4 N in dioxane); (c) 2-(1*H*-imidazol-5-yl)acetic acid hydrochloride, HATU, *N,N*-diisopropylethylamine, DMF; (d) H₂, Pd/C, MeOH; (e) benzaldehyde, MeOH, NaBH(OAc)₃.

and Boc deprotection provided **50–52**. Finally, coupling with the appropriate carboxylic acid provided analogues **31–35**, **37**, and **38**. The synthesis outlined in Scheme 6 was utilized to provide >100 g of **37** for nonclinical toxicology studies.

Synthesis of the *cis* proline derivative **36**, shown in Scheme 7, started from commercially available (2*S*,4*R*)-1-(*tert*-butoxycarbonyl)-4-hydroxypyrrolidine-2-carboxylic acid (**54**) and in three steps was elaborated to give **55**. Oxidation of the alcohol followed by a Wittig reaction and reduction provided **36**.²²

Starting from *D*-pyroglutamic acid (**56**), ent-**37** was synthesized as shown in Scheme 8 in a manner similar to that for derivatives in Scheme 6, using the ethyl ester in place of *tert*-butyl to give **57** and carrying out the hydrolysis with lithium hydroxide. Orthogonal protection of the ester was advantageous in that it eliminated the requirement to add the Boc protecting group more than once during the synthesis.

Scheme 6^a

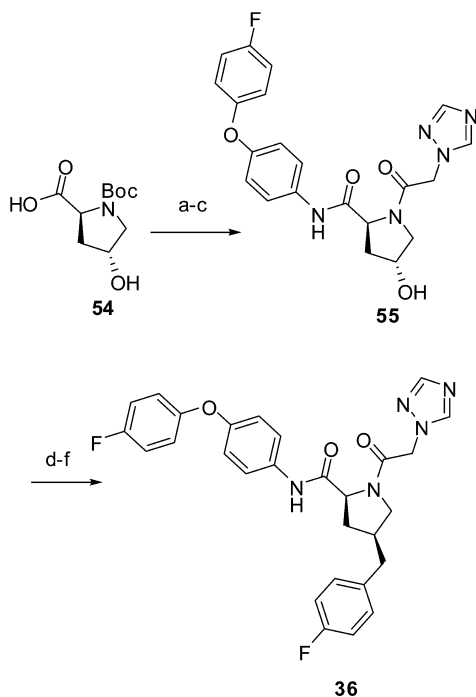
^aReagents: (a) *t*-BuOAc, HClO₄; (b) Boc₂O, *N,N*-diisopropylethylamine, CH₃CN; (c) LiHMDS, THF, R-Br, -78 °C; (d) LiBEt₃H, THF, -78 °C; (e) Et₃SiH, BF₃·Et₂O, CH₂Cl₂, -78 °C; (f) TFA, CH₂Cl₂, -78 °C; (g) Boc₂O, *N,N*-diisopropylethylamine, dioxane, CH₃CN; (h) 4-(4-fluorophenoxy)aniline or 4-phenoxyaniline, HATU, *N,N*-diisopropylethylamine, DMF; (i) TFA, CH₂Cl₂; (j) R'CH₂COOH, HATU, *N,N*-diisopropylethylamine, DMF.

CONCLUSIONS

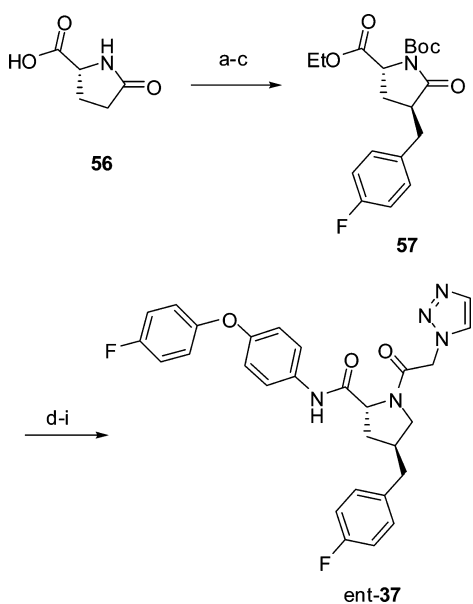
A series of novel and highly potent S1P₁ antagonists based on the serine and proline structural motif were disclosed. The incorporation of different functional groups on the periphery of HTS hit **1** had a profound impact on the activity. Further optimization of the serine series led us to explore more constrained analogues such as proline **34** which provided increased potency and greatly improved mouse oral exposure. In efforts to improve the CYP profile of **34**, analogues such as **37** and **38** were synthesized, and further evaluation of these agents demonstrated that similar efficacy could be achieved at lower doses than comparable serine analogues. In addition, oral administration of **37** shows excellent pharmacokinetics in multiple species. Further studies demonstrating the pharmacological profile of **37** will be published in due course.

EXPERIMENTAL SECTION

All reagents and solvents employed were purchased commercially and used without further purification unless otherwise indicated. Melting points were determined on a Melt-Temp melting point apparatus model II and are uncorrected. NMR spectra were recorded on a Varian Mercury Plus 400 MHz instrument. ¹³C NMR spectra are assigned with peaks "as observed" with no comment on splitting patterns. Reported spectra may appear to contain superfluous signals due to the existence of rotamers and/or carbon-fluorine coupling. Chemical

Scheme 7^a

^aReagents: (a) HATU, DMF, *N,N*-diisopropylethylamine, 4-(4-fluorophenoxy)aniline; (b) HCl (4 N in dioxane); (c) 2-(1*H*-1,2,4-triazol-1-yl)acetic acid, HATU, *N,N*-diisopropylethylamine, DMF; (d) DMSO, (COCl)₂, CH₂Cl₂, DCM, NEt₃, -78 °C; (e) 4-fluorobenzyltriphenylphosphine chloride, DMSO, NaH, 70 °C; (f) Pd/C (10%), MeOH, H₂.

Scheme 8^a

^aReagents: (a) TsOH; (b) Boc₂O, *N,N*-diisopropylethylamine, CH₃CN; (c) LiHMDS, THF, 1-(bromomethyl)-4-fluorobenzene, -78 °C; (d) LiBEt₃H, THF, -78 °C; (e) Et₃SiH, BF₃·Et₂O, CH₂Cl₂, -78 °C; (f) KOH, MeOH; (g) 4-(4-fluorophenoxy)aniline, HATU, *N,N*-diisopropylethylamine, DMF; (h) TFA, CH₂Cl₂; (i) 2-(1*H*-1,2,3-triazol-1-yl)acetic acid, HATU, *N,N*-diisopropylethylamine, DMF.

shifts are reported in parts per million (ppm) relative to an internal standard of tetramethylsilane in deuterated dimethylsulfoxide (DMSO-*d*₆) or deuterated chloroform (CDCl₃). Elemental analyses were

conducted by Robertson Microlit Laboratories, Madison, NJ. Positive ion FAB high resolution mass spectrometry was conducted by Analytical Instrument Group, Inc., Raleigh, NC. All final compounds were purified to ≥95% purity as assayed by analytical HPLC (YMC-Pack Pro 150 mm × 4.6 mm, 5 μm C18 column, Shimadzu LC-10AT VP system equipped with a Shimadzu SPD-M10A VP diode array detector) at a 1.5 mL/min flow rate with a gradient of 5–95% acetonitrile (containing 0.1% TFA) in 0.1% aqueous TFA for 25 min and total run time of 27 min.

***N*-(2-(3-(Benzyloxy)-1-oxo-1-(4-phenoxyphenylamino)propan-2-ylamino)-2-oxoethyl)-*N*-methylbenzamide (1).** To a flask charged with **39** (5.00 g, 16.9 mmol) were added HATU (7.00 g, 18.6 mmol) and *N,N*-diisopropylethylamine (8.80 mL, 50.7 mmol). After the mixture was stirred for 15 min 4-phenoxyaniline (3.40 g, 18.6 mmol) was added, and the mixture was stirred at room temperature for 18 h. The reaction mixture was partitioned between ethyl acetate and water. The aqueous layer was separated and extracted twice with ethyl acetate. The combined extracts were washed sequentially with 5% lithium chloride (3×), 1 N sodium bicarbonate (2×), 5% citric acid (2×), water (2×), brine and then dried over anhydrous sodium sulfate, filtered, and concentrated in vacuo. The crude material was recrystallized from methanol to afford a colorless solid. The solid was combined with HCl (25 mL, 4 N in dioxane). The mixture was stirred at room temperature for 18 h. Volatiles then were removed in vacuo, and the resultant oil was partitioned between 1 N sodium bicarbonate and ethyl acetate. The aqueous layer was extracted with ethyl acetate. The combined extracts were washed with brine (2×), dried over anhydrous sodium sulfate, filtered, and concentrated in vacuo. The crude product was recrystallized from methanol to give **rac-41** (2.00 g, 5.47 mmol, 33% yield) as an off-white solid. ¹H NMR (400 MHz, CDCl₃) δ 9.55 (s, 1H), 7.60–7.50 (m, 2H), 7.40–7.27 (m, 8H), 7.09–7.07 (m, 1H), 7.01–6.95 (m, 3H), 4.58–4.56 (m, 2H), 3.85–3.70 (m, 3H), 1.98–1.96 (m, 2H). MS (EI) for C₂₂H₂₂N₂O₃, found 363.0 (MH⁺).

To a flask charged with 2-amino-3-benzyloxy-*N*-(4-phenoxyphenyl)propanamide (**rac-41**) (150 mg, 0.420 mmol) were added 2-(*N*-methylbenzamido)acetic acid (97 mg, 0.50 mmol), HATU (188 mg, 0.500 mmol), DMF (1 mL), and *N,N*-diisopropylethylamine (370 μL, 2.10 mmol), and the mixture was stirred at room temperature for 18 h. The reaction mixture was partitioned between ethyl acetate and water. The aqueous layer was separated and extracted with ethyl acetate. The combined organic layer was washed with 5% lithium chloride (3×), 1 N sodium bicarbonate (2×), water (2×), then concentrated in vacuo. Product was purified from the residue by reverse phase HPLC. The purified product was taken up into methanol and the solution was neutralized with basic resin, filtered, and concentrated in vacuo to provide *N*-(2-(3-(benzyloxy)-1-oxo-1-(4-phenoxyphenylamino)propan-2-ylamino)-2-oxoethyl)-*N*-methylbenzamide (**1**) (32 mg, 14% yield) as a colorless solid. ¹H NMR (400 MHz, CDCl₃) δ 8.80 (s, 1H), 7.63–7.30 (m, 13H), 7.11–6.92 (m, 5H), 4.74–4.71 (m, 1H), 4.61–4.59 (m, 2H), 4.28–4.15 (m, 1H), 4.10–4.00 (m, 1H), 3.73–3.67 (m, 2H), 3.17 (s, 3H). MS (EI) for C₃₂H₃₁N₃O₅, found 538.0 (MH⁺).

Compounds **2–24**, **27**, and **28** were prepared according to a similar procedure as described for the synthesis of compound **1**.

(*R*)-*N*-(2-(3-(Benzyloxy)-1-oxo-1-(4-phenoxyphenylamino)propan-2-ylamino)-2-oxoethyl)-*N*-methylbenzamide (2). ¹H NMR (400 MHz, CDCl₃) δ 8.80 (s, 1H), 7.63–7.30 (m, 13H), 7.11–6.92 (m, 5H), 4.74–4.71 (m, 1H), 4.61–4.59 (m, 2H), 4.28–4.15 (m, 1H), 4.10–4.00 (m, 1H), 3.73–3.67 (m, 2H), 3.17 (s, 3H). MS (EI) for C₃₂H₃₁N₃O₅, found 538.0 (MH⁺).

(*S*)-*N*-(2-(3-(Benzyloxy)-1-oxo-1-(4-phenoxyphenylamino)propan-2-ylamino)-2-oxoethyl)-*N*-methylbenzamide (3). ¹H NMR (400 MHz, CDCl₃) δ 8.80 (s, 1H), 7.63–7.30 (m, 13H), 7.11–6.92 (m, 5H), 4.73–4.72 (m, 1H), 4.61–4.59 (m, 2H), 4.28–4.15 (m, 1H), 4.10–4.00 (m, 1H), 3.72–3.70 (m, 2H), 3.17 (s, 3H). MS (EI) for C₃₂H₃₁N₃O₅, found 538.0 (MH⁺).

***N*-(3-(Benzyloxy)-1-oxo-1-(4-phenoxyphenylamino)propan-2-yl)-5-oxo-5-(thiophen-2-yl)pentanamide (4).** ¹H NMR (400 MHz, DMSO-*d*₆) δ 10.19 (s, 1H), 8.27 (d, *J* = 7.8 Hz, 1H), 7.98 (dd, *J* = 4.9, 1.1 Hz, 1H), 7.90 (dd, *J* = 3.8, 1.1 Hz, 1H), 7.70–7.50 (m, 2H),

7.41–7.32 (m, 2H), 7.33–7.23 (m, 5H), 7.20 (dd, $J = 4.9, 3.8$ Hz, 1H), 7.10 (tt, $J = 7.6, 1.0$ Hz, 1H), 7.04–6.90 (m, 4H), 4.72 (q, $J = 6.2$ Hz, 1H), 4.52 (s, 2H), 3.72–3.57 (m, 2H), 2.96 (dd, $J = 7.7, 5.7$ Hz, 2H), 2.26 (t, $J = 7.4$ Hz, 2H), 1.95–1.74 (m, 2H). MS (EI) for $C_{31}H_{30}N_2O_5S$, found 543.7 (MH⁺).

N-(3-(Benzyloxy)-1-oxo-1-(4-phenoxyphenylamino)propan-2-yl)cyclopropanecarboxamide (5). ¹H NMR (400 MHz, CDCl₃) δ 7.75–7.34 (m, 9H), 7.10–7.06 (m, 1H), 6.98–6.95 (m, 4H), 4.89–4.87 (m, 1H), 4.70–4.62 (m, 2H), 4.16–4.14 (m, 1H), 3.75–3.70 (m, 1H), 1.14–0.60 (m, 5H). MS (EI) for $C_{26}H_{26}N_2O_4$, found 431.5 (MH⁺).

(S)-N-(3-(Benzyloxy)-1-oxo-1-(4-phenoxyphenylamino)propan-2-yl)-1H-imidazole-5-carboxamide (6). ¹H NMR (400 MHz, CDCl₃) δ 9.54 (s, 1H), 8.52 (s, 1H), 7.98 (d, $J = 7.5$ Hz, 1H), 7.73 (s, 1H), 7.65 (s, 1H), 7.47–7.43 (m, 2H), 7.35–7.31 (m, 6H), 7.10–7.06 (m, 1H), 6.99–6.96 (m, 4H), 4.91–4.88 (m, 1H), 4.69 (d, $J = 11.8$ Hz, 1H), 4.62 (d, $J = 11.8$ Hz, 1H), 4.13 (dd, $J = 9.3, 4.3$ Hz, 1H), 3.78 (dd, $J = 9.4, 6.7$ Hz, 1H). MS (EI) for $C_{26}H_{24}N_4O_4$, found 456.9 (MH⁺).

(S)-2-(2-(1H-Imidazol-5-yl)acetamido)-3-(benzyloxy)-N-(4-phenoxyphenyl)propanamide (7). ¹H NMR (400 MHz, CDCl₃) δ 9.23 (s, 1H), 7.53–7.40 (m, 4H), 7.35–7.27 (m, 6H), 7.08 (t, $J = 8.0$ Hz, 1H), 7.00–6.92 (m, 4H), 6.87 (s, 1H), 4.78–4.75 (m, 1H), 4.60 (d, $J = 11.8$ Hz, 1H), 4.52 (d, $J = 11.8$ Hz, 1H), 4.18 (dd, $J = 9.3, 3.7$ Hz, 1H), 3.66 (dd, $J = 9.4, 5.8$ Hz, 1H), 3.61 (d, $J = 3.8$ Hz, 2H). MS (EI) for $C_{27}H_{26}N_4O_4$, found 471.0 (MH⁺).

(S)-3-(Benzyloxy)-2-(2-(1-methyl-1H-imidazol-4-yl)acetamido)-N-(4-phenoxyphenyl)propanamide (8). ¹H NMR (400 MHz, CDCl₃) δ 9.25 (s, 1H), 7.51–7.34 (m, 3H), 7.35–7.30 (m, 7H), 7.10–7.09 (m, 1H), 6.99–6.96 (m, 4H), 6.79 (s, 1H), 4.79–4.75 (m, 1H), 4.63 (d, $J = 11.8$ Hz, 1H), 4.53 (d, $J = 11.8$ Hz, 1H), 4.14 (dd, $J = 9.3, 3.5$ Hz, 1H), 3.68–3.65 (m, 1H), 3.64 (s, 3H), 3.59 (d, $J = 3.2$ Hz, 2H). MS (EI) for $C_{28}H_{28}N_4O_4$, found 485.3 (MH⁺).

(S)-3-(Benzyloxy)-2-(2-(2,5-dichlorophenyl)acetamido)-N-(4-phenoxyphenyl)propanamide (9). ¹H NMR (400 MHz, DMSO-*d*₆) δ 10.23 (s, 1H), 8.61 (d, $J = 7.9$ Hz, 1H), 7.63 (d, $J = 9.0$ Hz, 2H), 7.50 (d, $J = 2.6$ Hz, 1H), 7.45 (d, $J = 9.0$ Hz, 1H), 7.41–7.24 (m, 8H), 7.14–7.06 (m, 1H), 7.02 (d, $J = 9.0$ Hz, 2H), 6.97 (d, $J = 7.7$ Hz, 2H), 4.74 (dd, $J = 13.9, 6.1$ Hz, 1H), 4.54 (s, 2H), 3.73 (s, 2H), 3.71–3.65 (m, 2H). MS (EI) for $C_{30}H_{26}Cl_2N_2O_4$, found 549.3 (MH⁺).

(S)-3-(Benzyloxy)-2-(2-(2-fluorophenyl)acetamido)-N-(4-phenoxyphenyl)propanamide (10). ¹H NMR (400 MHz, CDCl₃) δ 8.43 (s, 1H), 7.40–7.22 (m, 11H), 7.18–7.04 (m, 3H), 7.01–6.89 (m, 3H), 6.60 (d, $J = 6.6$ Hz, 1H), 4.76–4.68 (m, 1H), 4.64–4.47 (m, 2H), 4.03–3.95 (m, 1H), 3.66 (s, 2H), 3.61–3.54 (m, 1H). MS (EI) for $C_{30}H_{27}FN_2O_4$, found 498.9 (MH⁺).

(S)-2-(2-(1H-Imidazol-5-yl)acetamido)-3-(benzyloxy)-N-(3-chloro-4-phenoxyphenyl)propanamide (11). ¹H NMR (400 MHz, DMSO-*d*₆) δ 10.41 (s, 1H), 8.45 (d, $J = 10.0$ Hz, 1H), 7.95 (s, 1H), 7.59 (s, 1H), 7.49 (dd, $J = 8.9, 2.6$ Hz, 1H), 7.36–7.25 (m, 7H), 7.13 (d, $J = 8.9$ Hz, 1H), 7.09–7.06 (m, 1H), 6.89 (d, $J = 7.7$ Hz, 2H), 4.68–4.61 (m, 1H), 4.50 (s, 2H), 3.73–3.32 (m, 4H). MS (EI) for $C_{27}H_{25}ClN_4O_4$, found 504.9 (MH⁺).

(S)-2-(2-(1H-Imidazol-5-yl)acetamido)-3-(benzyloxy)-N-(4-(4-chlorophenoxy)phenyl)propanamide (12). ¹H NMR (400 MHz, DMSO-*d*₆) δ 11.95 (br s, 1H), 10.28 (s, 1H), 8.45 (d, $J = 7.4$ Hz, 1H), 7.66–7.63 (m, 3H), 7.43–7.39 (m, 2H), 7.33–7.25 (m, 4H), 7.05–6.98 (m, 5H), 4.72–4.65 (m, 1H), 4.51 (s, 2H), 3.73–3.63 (m, 2H), 3.54–3.40 (m, 2H). MS (EI) for $C_{27}H_{25}ClN_4O_4$, found 505.0 (MH⁺).

(S)-2-(2-(1H-Imidazol-5-yl)acetamido)-3-(benzyloxy)-N-(4-(3-chlorophenoxy)phenyl)propanamide (13). ¹H NMR (400 MHz, DMSO-*d*₆) δ 10.32 (s, 1H), 8.48 (d, $J = 7.8$ Hz, 1H), 7.68 (d, $J = 9.0$ Hz, 2H), 7.60 (s, 1H), 7.41–7.36 (t, $J = 8.2$ Hz, 1H), 7.34–7.25 (m, 5H), 7.17–7.15 (dd, $J = 7.6, 2.2$ Hz, 1H), 7.09–7.07 (d, $J = 9.0$ Hz, 2H), 7.02–6.98 (m, 1H), 6.94–6.91 (m, 2H), 4.71–4.66 (m, 1H), 4.52 (s, 2H), 3.73–3.64 (m, 2H), 3.52–3.39 (m, 2H). MS (EI) for $C_{27}H_{25}ClN_4O_4$, found 505.0 (MH⁺).

(S)-2-(2-(1H-Imidazol-5-yl)acetamido)-3-(benzyloxy)-N-(4-(2-chlorophenoxy)phenyl)propanamide (14). ¹H NMR (400 MHz, DMSO-*d*₆) δ 11.95 (s, 1H), 10.26 (s, 1H), 8.43 (d, $J = 8.4$ Hz, 1H), 7.78–7.45 (m, 4H), 7.44–7.23 (m, 6H), 7.23–7.11 (m, 1H), 7.11–6.85 (m, 4H), 4.77–4.58 (m, 1H), 4.51 (s, 2H), 3.77–3.40 (m, 4H). MS (EI) for $C_{27}H_{25}ClN_4O_4$, found 505.0 (MH⁺).

(S)-2-(2-(1H-Imidazol-5-yl)acetamido)-3-(benzyloxy)-N-(4-(4-fluorophenoxy)phenyl)propanamide (15). ¹H NMR (400 MHz, DMSO-*d*₆) δ 11.94 (s, 1H), 10.23 (s, 1H), 8.43 (d, $J = 8.6$ Hz, 1H), 7.63–7.61 (m, 2H), 7.31–7.14 (m, 9H), 7.04–6.94 (m, 4H), 4.70–4.64 (m, 1H), 4.51 (s, 2H), 3.73–3.63 (m, 2H), 3.54–3.25 (m, 2H). MS (EI) for $C_{27}H_{25}FN_4O_4$, found 489.3 (MH⁺).

(S)-2-(2-(1H-Imidazol-5-yl)acetamido)-3-(benzyloxy)-N-(4-(cyclohexyloxy)phenyl)propanamide (16). ¹H NMR (400 MHz, CDCl₃) δ 8.95 (s, 1H), 7.70–7.50 (m, 2H), 7.37–7.25 (m, 7H), 6.96–6.87 (m, 3H), 4.79–4.73 (m, 1H), 4.64–4.61 (m, 2H), 4.17–4.10 (m, 2H), 3.68–3.59 (m, 3H), 1.80–1.20 (m, 10H). MS (EI) for $C_{27}H_{32}N_4O_4$, found 477.0 (MH⁺).

(S)-2-(2-(1H-Imidazol-5-yl)acetamido)-3-(benzyloxy)-N-(4-(benzyloxy)phenyl)propanamide (17). ¹H NMR (400 MHz, CDCl₃) δ 7.55 (s, 1H), 7.44–7.37 (m, 6H), 7.35–7.26 (m, 6H), 6.94–6.90 (m, 3H), 5.05 (s, 2H), 4.71 (dd, $J = 5.0, 4.6$ Hz, 1H), 4.58 (d, $J = 11.8$ Hz, 1H), 4.51 (d, $J = 11.8$ Hz, 1H), 3.98 (dd, $J = 9.2, 3.9$ Hz, 1H), 3.66 (dd, $J = 9.4, 5.6$ Hz, 1H), 3.60 (s, 2H). MS (EI) for $C_{28}H_{28}N_4O_4$, found 485.2 (MH⁺).

(S)-2-(2-(1H-Imidazol-5-yl)acetamido)-3-(benzyloxy)-N-(dibenzol[b,d]furan-2-yl)propanamide (18). ¹H NMR (400 MHz, DMSO-*d*₆) δ 11.96 (s, 1H), 10.54 (s, 1H), 8.48 (d, $J = 7.9$ Hz, 1H), 8.17 (d, $J = 1.5$ Hz, 1H), 8.07 (dd, $J = 8.0, 2.5$ Hz, 2H), 7.68 (d, $J = 8.2$ Hz, 1H), 7.61 (s, 1H), 7.52–7.45 (m, 2H), 7.40 (s, 1H), 7.32–7.21 (m, 4H), 6.93 (s, 1H), 4.75 (dd, $J = 11.4, 6.1$ Hz, 1H), 4.52 (s, 2H), 3.88–3.62 (m, 2H), 3.52–3.41 (m, 2H). MS (EI) for $C_{27}H_{24}N_4O_4$, found 469.0 (MH⁺).

(S)-2-(2-(1H-Imidazol-5-yl)acetamido)-3-(benzyloxy)-N-(4-benzyloxyphenyl)propanamide (19). ¹H NMR (400 MHz, CDCl₃) δ 11.95 (s, 1H), 10.14 (s, 1H), 8.39 (d, $J = 7.9$ Hz, 1H), 7.61 (s, 1H), 7.52 (d, $J = 14.1$ Hz, 1H), 7.30–7.15 (m, 11H), 6.96 (s, 1H), 4.71–4.64 (m, 1H), 4.49 (s, 2H), 3.89 (s, 2H), 3.71–3.61 (m, 2H), 3.51–3.32 (m, 2H). MS (EI) for $C_{28}H_{28}N_4O_3$, found 469.3 (MH⁺).

(S)-2-(2-(1H-Imidazol-5-yl)acetamido)-3-(benzyloxy)-N-(4-(phenylamino)phenyl)propanamide (20). ¹H NMR (400 MHz, DMSO-*d*₆) δ 10.08 (s, 1H), 8.39 (d, $J = 10.4$ Hz, 1H), 8.08 (s, 1H), 7.62 (s, 1H), 7.48 (d, $J = 7.5$ Hz, 2H), 7.43–7.26 (m, 4H), 7.21 (dd, $J = 19.4, 10.6$ Hz, 2H), 7.10–6.93 (m, 4H), 6.77 (d, $J = 8.1$ Hz, 1H), 4.81–4.57 (m, 1H), 4.51 (s, 1H), 3.82–3.53 (m, 2H), 3.54–3.36 (m, 3H). MS (EI) for $C_{27}H_{27}N_3O_3$, found 470.3 (MH⁺).

(S)-2-(2-(1H-Imidazol-5-yl)acetamido)-3-(benzyloxy)-N-(biphenyl-4-yl)propanamide (21). ¹H NMR (400 MHz, DMSO-*d*₆) δ 11.97 (s, 1H), 10.31 (s, 1H), 8.46 (d, $J = 7.8$ Hz, 1H), 7.81–7.57 (m, 7H), 7.45 (t, $J = 7.7$ Hz, 2H), 7.37–7.15 (m, 6H), 4.82–4.62 (m, 1H), 4.50 (s, 2H), 3.81–3.53 (m, 2H), 3.53–3.36 (m, 2H). MS (EI) for $C_{27}H_{26}N_4O_3$, found 455.0 (MH⁺).

(S)-2-(2-(1H-Imidazol-5-yl)acetamido)-N-(4-phenoxyphenyl)-5-phenylpentanamide (22). ¹H NMR (400 MHz, CDCl₃) δ 9.17 (s, 1H), 7.54 (d, $J = 7.9$ Hz, 1H), 7.48 (s, 1H), 7.46–7.39 (m, 2H), 7.35–7.20 (m, 4H), 7.20–7.01 (m, 4H), 6.95–6.88 (m, 3H), 6.81 (s, 1H), 4.60 (dd, $J = 13.8, 7.6$ Hz, 1H), 3.66–3.42 (m, 2H), 2.71–2.50 (m, 2H), 2.08–1.92 (m, 1H), 1.87–1.61 (m, 3H). MS (EI) for $C_{28}H_{28}N_4O_3$, found 469.5 (MH⁺).

(S)-2-(2-(1H-Imidazol-5-yl)acetamido)-N-(4-(4-chlorophenoxy)phenyl)propanamide (23). ¹H NMR (400 MHz, DMSO-*d*₆) δ 11.94 (s, 1H), 10.12 (s, 1H), 8.37 (d, $J = 7.3$ Hz, 1H), 7.72–7.55 (m, 3H), 7.48–7.33 (m, 2H), 7.06–7.01 (m, 2H), 7.01–6.95 (m, 2H), 6.90 (s, 1H), 4.53–4.22 (m, 1H), 3.47–4.37 (m, 2H), 1.32 (s, 3H). MS (EI) for $C_{26}H_{19}ClN_3O_3$, found 455.0 (MH⁺).

(S)-2-(2-(1H-Imidazol-5-yl)acetamido)-N-(4-(4-chlorophenoxy)phenyl)-3-phenylpropanamide (24). ¹H NMR (400 MHz, DMSO-*d*₆) δ 11.98 (s, 1H), 10.25 (s, 1H), 8.43 (d, $J = 8.1$ Hz, 1H), 7.68–7.49 (m, 3H), 7.49–7.31 (m, 2H), 7.35–7.13 (m, 5H), 7.09–6.87 (m, 4H), 6.80 (s, 1H), 4.65 (td, $J = 9.0, 5.1$ Hz, 1H), 3.40 (d, $J = 15.5$ Hz, 1H), 3.33 (d, $J = 15.5$ Hz, 1H), 3.07 (dd, $J = 27.9, 14.0$ Hz, 1H), 2.88 (dd, $J = 13.7, 9.3$ Hz, 1H). MS (EI) for $C_{26}H_{23}ClN_4O_3$, found 475.9 (MH⁺).

(S)-2-(2-(1H-Imidazol-5-yl)-N-methylacetamido)-3-(benzyloxy)-N-(4-phenoxyphenyl)propanamide (27). ¹H NMR (400 MHz, DMSO-*d*₆, mixture of rotamers observed) δ 12.30–11.90 (m, 1H), 10.20 (s, 1H), 7.94–7.09 (m, 16H), 5.35–5.30 (m, 1H), 4.62–4.48

(m, 2H), 4.04–3.59 (m, 1H), 3.41 (d, $J = 14.4$ Hz, 1H), 3.08 (s, 3H), 2.70 (s, 2H). MS (EI) for $C_{28}H_{28}N_4O_4$, found 485.2 (MH^+).

(S)-2-(2-(1H-imidazol-5-yl)acetamido)-3-(benzyloxy)-N-methyl-N-(4-phenoxyphenyl)propanamide (28). 1H NMR (400 MHz, $CDCl_3$) δ 7.59–7.20 (m, 9H), 7.17 (t, $J = 7.4$ Hz, 1H), 7.12–6.74 (m, 5H), 6.76–6.07 (m, 1H), 4.80 (dd, $J = 12.2, 4.9$ Hz, 1H), 4.48 (d, $J = 12.1$ Hz, 1H), 4.31 (d, $J = 12.1$ Hz, 1H), 3.67–3.47 (m, 3H), 3.42 (dd, $J = 9.7, 5.2$ Hz, 1H), 3.22 (s, 3H). MS (EI) for $C_{28}H_{28}N_4O_3$, found 485.0 (MH^+).

(R)-N-(2-(Benzyloxy)-1-(5-(4-fluorophenoxy)-1H-benzo[d]-imidazol-2-yl)ethyl)-2-(1H-imidazol-5-yl)acetamide (29). A mixture of 5-chloro-2-nitroaniline (345 mg, 2.00 mmol), 4-fluorophenol (224 mg, 2.00 mmol), K_2CO_3 (549 mg, 4.00 mmol), and DMF (8 mL) was stirred at 120 °C for 24 h. After the mixture was cooled, water was added and the mixture was extracted with ethyl acetate (4 \times). The combined organic layers were dried over anhydrous magnesium sulfate, concentrated, and purified by flash chromatography (hexanes/ethyl acetate (6:1)) to give 5-(4-fluorophenoxy)-2-nitroaniline (510 mg, quant) as a yellow powder.

A mixture of 5-(4-fluorophenoxy)-2-nitroaniline (410 mg, 1.65 mmol), ammonium formate (520 mg, 8.26 mmol), 10% Pd/C (123 mg, 0.116 mmol), and methanol (10 mL) was stirred at room temperature for 30 min. After filtration, the filtrate was concentrated and the residue was purified by flash chromatography (hexanes/ethyl acetate (2:3 to 1:2)) to give 43 (370 mg, quant) as a brown oil.

To a stirred solution of 43 (370 mg, 1.70 mmol), 39 (550 mg, 1.86 mmol), and DMF (4 mL) were added *N,N*-diisopropylethylamine (0.880 mL, 5.10 mmol) and HATU (750 mg, 2.00 mmol) at room temperature. After the mixture was stirred for 1 h, saturated sodium bicarbonate was added and the resulting solution was extracted with ethyl acetate (4 \times). The combined organic layers were dried over anhydrous magnesium sulfate, concentrated, and purified by flash chromatography (hexanes/ethyl acetate (3:1 to 2:1)) to give (*S*)-*tert*-butyl 1-(2-amino-4-(4-fluorophenoxy)phenylamino)-3-(benzyloxy)-1-oxopropan-2-ylcarbamate (610 mg, 72%) as a brown foam.

A mixture of (*S*)-*tert*-butyl 1-(2-amino-4-(4-fluorophenoxy)phenylamino)-3-(benzyloxy)-1-oxopropan-2-ylcarbamate (610 mg, 1.23 mmol) and AcOH (6 mL) was stirred at 60 °C for 1 h. After removal of acetic acid in vacuo, HCl (4 mL, 4 N in dioxane) was added and the resulting solution was stirred at room temperature for 30 min. After concentration, the residue was purified by reverse phase HPLC to give (*R*)-2-(benzyloxy)-1-(5-(4-fluorophenoxy)-1H-benzo[d]imidazol-2-yl)ethanamine (250 mg, 54%) as a pale yellow foam.

To a stirred solution of (*R*)-2-(benzyloxy)-1-(5-(4-fluorophenoxy)-1H-benzo[d]imidazol-2-yl)ethanamine (150 mg, 0.397 mmol), 4-imidazoleacetic acid hydrochloride (84.0 mg, 0.517 mmol), and DMF (1.5 mL) were added *N,N*-diisopropylethylamine (0.350 mL, 1.99 mmol) and HATU (226 mg, 0.596 mmol) at room temperature. After the mixture was stirred for 30 min, saturated sodium bicarbonate was added and the resulting solution was extracted with ethyl acetate (4 \times). The combined organic layers were dried over anhydrous magnesium sulfate, concentrated, and purified by reverse phase HPLC to give 29 (75 mg, 39%) as a white powder after lyophilization. 1H NMR (400 MHz, $DMSO-d_6$) δ 12.43 (br s, 1H), 8.75 (d, $J = 8.1$ Hz, 1H), 7.77 (s, 1H), 7.56 (d, $J = 8.6$ Hz, 1H), 7.33–7.25 (m, 5H), 7.20–7.16 (m, 3H), 7.00–6.96 (m, 3H), 6.89 (dd, $J = 8.7, 2.3$ Hz, 1H), 5.35–5.30 (m, 1H), 4.52 (s, 2H), 3.93 (dd, $J = 9.8, 5.1$ Hz, 1H), 3.86 (dd, $J = 9.8, 7.0$ Hz, 1H), 3.55 (d, $J = 15.2$ Hz, 1H), 3.48 (d, $J = 15.2$ Hz, 1H). MS (EI) for $C_{27}H_{24}FN_5O_3$, found 486.2 (MH^+).

(S)-1-(2-(1H-imidazol-5-yl)acetyl)-4-benzyl-N-(4-(4-fluorophenoxy)phenyl)piperazine-2-carboxamide (30). A flask was charged with 44 (1.00 g, 2.74 mmol), 4-(4-fluorophenoxy)aniline (558 mg, 2.75 mmol), *N,N*-diisopropylethylamine (3.00 mL, 17.3 mmol), HATU (1.15 g, 3.03 mmol), and DMF (8 mL). The reaction mixture was stirred at room temperature for 20 min, at which time it was quenched with saturated sodium bicarbonate and extracted with ethyl acetate. The organic layer was separated, washed with water, brine, dried over anhydrous sodium sulfate, filtered, and concentrated to provide (*S*)-4-benzyl 1-*tert*-butyl 2-(4-(4-fluorophenoxy)phenylcarbamoyl)piperazine-1,4-dicarboxylate (1.46 g, quant) as an off-white solid.

A flask was charged with (*S*)-4-benzyl 1-*tert*-butyl 2-(4-(4-fluorophenoxy)phenylcarbamoyl)piperazine-1,4-dicarboxylate (1.46 g, 2.75 mmol) and HCl (10 mL, 4 N in dioxane). The mixture was stirred at room temperature for 1 h, at which time it was quenched with saturated sodium bicarbonate and extracted with ethyl acetate. The organic layer was separated, washed with water, brine, dried over anhydrous sodium sulfate, filtered, and concentrated to provide (*S*)-benzyl 3-(4-(4-fluorophenoxy)phenylcarbamoyl)piperazine-1-carboxylate (1.08 g, 88%) as an off-white solid.

A flask was charged with (*S*)-benzyl 3-(4-(4-fluorophenoxy)phenylcarbamoyl)piperazine-1-carboxylate (1.08 g, 2.41 mmol), 4-imidazoleacetic acid hydrochloride (392 mg, 2.41 mmol), *N,N*-diisopropylethylamine (1.0 mL, 5.8 mmol), HATU (1.01 g, 2.65 mmol), and DMF (5 mL). The reaction mixture was stirred at room temperature for 20 min, at which time it was quenched with saturated sodium bicarbonate and extracted with ethyl acetate. The organic layer was separated, washed with water, brine, dried over anhydrous sodium sulfate, filtered, and concentrated. The residue was purified by reverse phase HPLC to provide 45 (0.80 g, 67% yield) as an off-white solid. 1H NMR (400 MHz, $CDCl_3$) δ 10.27 (s, 1H), 9.18 (s, 1H), 7.60–7.49 (m, 3H), 7.47–7.21 (m, 5H), 7.06–6.91 (m, 6H), 5.45 (s, 1 H), 5.17 (s, 2H), 5.09–5.00 (m, 2H), 4.09–3.97 (m, 2H), 3.81–3.73 (m, 2H), 3.46–3.37 (m, 1H), 3.17 (dd, $J = 12.6, 4.3$ Hz, 1H), 3.13–3.00 (m, 1H). MS (EI) for $C_{30}H_{28}FN_5O_5$, found

A flask was charged with 45 (0.80 g, 1.4 mmol), methanol (10 mL), and Pd/C (10%, 100 mg). The mixture was stirred under a hydrogen atmosphere (balloon) for 14 h, at which time it was exposed to air, filtered through Celite, and concentrated. The residue was purified by reverse phase HPLC to yield (*S*)-1-(2-(1H-imidazol-5-yl)acetyl)-*N*-(4-(4-fluorophenoxy)phenyl)piperazine-2-carboxamide (0.50 g, 83% yield) as an off-white solid. 1H NMR (400 MHz, $CDCl_3$) δ 10.02 (s, 1H), 9.20 (s, 1H), 7.63–7.56 (m, 2H), 7.52 (s, 1H), 7.05–6.93 (m, 6H), 5.34 (s, 1 H), 4.05–4.00 (m, 1H), 3.94–3.86 (m, 1H), 3.78–3.71 (m, 2H), 3.28–3.20 (m, 1H), 3.00–2.94 (m, 1H), 2.89–2.74 (m, 2H), 2.61–2.53 (m, 1H). MS (EI) for $C_{22}H_{22}FN_5O_3$, found 424.2 (MH^+).

A flask was charged with (*S*)-1-(2-(1H-imidazol-5-yl)acetyl)-*N*-(4-(4-fluorophenoxy)phenyl)piperazine-2-carboxamide (107 mg, 0.252 mmol), benzaldehyde (0.154 mL, 1.51 mmol), methanol (10 mL), and $NaBH_4(OAc)_3$ (534 mg, 2.52 mmol). The reaction mixture was stirred at room temperature for 30 min, at which time it was diluted with water and washed with DCM. The aqueous layer was then basified with 2 N NaOH, extracted with ethyl acetate, washed with brine, dried over anhydrous sodium sulfate, filtered, and concentrated. The product (30) was yielded as an off-white solid (41 mg, 32% yield). 1H NMR (400 MHz, $CDCl_3$) δ 10.23 (s, 1H), 7.63–7.18 (m, 8H), 7.02–6.82 (m, 6H), 5.42 (s, 1 H), 4.02–3.90 (m, 1H), 3.88–3.80 (m, 1H), 3.78–3.61 (m, 2H), 3.58–3.34 (m, 2H), 3.08–2.97 (m, 1H), 2.78–2.64 (m, 1H), 2.28–2.18 (m, 1H), 2.11–2.00 (m, 1H). MS (EI) for $C_{29}H_{28}FN_5O_3$, found 514.3 (MH^+).

(2S,4R)-1-(2-(1H-1,2,3-Triazol-1-yl)acetyl)-4-(4-fluorobenzyl)-N-(4-(4-fluorophenoxy)phenyl)pyrrolidine-2-carboxamide (37). To a solution of L-pyroglutamic acid (46) (20.00 g, 154.9 mmol) in *tert*-butyl acetate (260 mL, 1.93 mol) at room temperature was added 70% aqueous perchloric acid (5 mL). The mixture was stirred for 18 h in a 500 mL round-bottom flask sealed with a rubber septum, then poured carefully into saturated sodium bicarbonate. The mixture was extracted with ethyl acetate (2 \times), dried over sodium sulfate, and concentrated in vacuo. The crude product solidified under high vacuum. The solid was treated with a mixture of hexanes/ether (10:1), filtered, and dried to give *tert*-butyl L-pyroglutamate (21.65 g, 75% yield) as a colorless solid.

The colorless solid obtained above (21.65 g, 116.9 mmol) was dissolved in acetonitrile (300 mL) with *N,N*-dimethylaminopyridine (1.29 g, 10.6 mmol) and cooled to 0 °C. A solution of di-*tert*-butyl-carbonate (33.20 g, 152.0 mmol) in acetonitrile (30 mL) was added slowly over 5 min. After 30 min the cooling bath was removed and the mixture was stirred at room temperature for 48 h. The mixture was concentrated in vacuo, and the residue was dissolved in ether (200 mL) and hexanes (200 mL). The organic phase was washed with saturated sodium bicarbonate (2 \times), saturated sodium chloride and dried over

anhydrous sodium sulfate. The solvent was removed in vacuo and the residue was passed through a short column of silica gel (eluted with hexanes/ethyl acetate, 4:1) to give a light yellow oil that solidified on standing. The solid thus obtained was treated with hexanes, filtered, and dried to give (S)-di-*tert*-butyl 5-oxopyrrolidine-1,2-dicarboxylate (24.22 g) as a pure colorless solid. The mother liquor was concentrated to give an additional crop (4.05 g) of colorless solid. The total yield of (S)-di-*tert*-butyl 5-oxopyrrolidine-1,2-dicarboxylate obtained in this manner was 85%. ^1H NMR (400 MHz, CDCl_3): δ 4.50–4.46 (m, 1H), 2.67–2.56 (m, 1H), 2.52–2.43 (m, 1H), 2.35–2.23 (m, 1H), 2.04–1.96 (m, 1H), 1.51 (s, 9H), 1.49 (s, 9H).

To a solution of (S)-di-*tert*-butyl 5-oxopyrrolidine-1,2-dicarboxylate (26.19 g, 91.79 mmol) in dry tetrahydrofuran (811 mL) at -78°C was added a solution of lithium bis(trimethylsilyl)amide (1 M in hexanes, 100.8 mL, 100.8 mmol) dropwise over 1 h under nitrogen. Upon completion of addition, the mixture was stirred for an additional 2 h at -78°C . Then a solution of 4-fluorobenzyl bromide (19.00 g, 100.8 mmol) in tetrahydrofuran (48 mL) was added over 10 min. The mixture was stirred at -78°C for 2 h, quenched with saturated ammonium chloride, and extracted with ether (2 \times). The combined organic layers were washed with saturated sodium chloride, dried over anhydrous sodium sulfate, and concentrated in vacuo. The crude mixture was purified by recrystallization from hexanes to give **49** (18.30 g) as a colorless solid. The mother liquor was purified by flash column chromatography (hexanes/ethyl acetate, 4:1) and recrystallized from hexanes to give an additional crop (4.90 g) of the colorless solid. The total yield of **49** obtained in this manner was 65%. ^1H NMR (400 MHz, CDCl_3): δ 7.14 (dd, $J = 8.4, 5.2$ Hz, 2H), 6.98 (t, $J = 8.6$ Hz, 2H), 4.35 (dd, $J = 9.0, 2.2$ Hz, 1H), 3.20 (dd, $J = 14.2, 4.2$ Hz, 1H), 2.92–2.84 (m, 1H), 2.71 (dd, $J = 13.8, 9.0$ Hz, 1H), 2.04–1.90 (m, 2H), 1.51 (s, 9H), 1.45 (s, 9H). ^{13}C NMR (100 MHz, CDCl_3): δ 174.6, 170.4, 163.2, 160.7, 149.5, 134.1, 134.1, 130.8, 130.7, 115.8, 159.6, 83.6, 82.6, 57.9, 43.6, 35.5, 28.2. MS (EI) for $\text{C}_{21}\text{H}_{28}\text{FNO}_5$: (392.2, MH^+). Mp: 99°C .

To a solution of **49** (23.20 g, 58.97 mmol) in dry tetrahydrofuran (200 mL) at -78°C was added a 1 M solution of lithium triethylborohydride in tetrahydrofuran (70.8 mL, 70.8 mmol) dropwise. After 30 min, the cooling bath was removed and saturated sodium bicarbonate was added. The reaction mixture was immersed in an ice–water bath, and 30% aqueous hydrogen peroxide (10 mL) was added. The mixture was stirred for 20 min at 0°C , then concentrated in vacuo to remove the tetrahydrofuran. The residue was diluted with water and extracted with dichloromethane (3 \times). The combined organic extracts were dried over sodium sulfate and concentrated in vacuo. The residue was dissolved in dichloromethane (200 mL) and triethylsilane (9.14 mL, 59.0 mmol). The solution was cooled to -78°C , and to this mixture was added boron trifluoride etherate (7.97 mL, 62.9 mmol) dropwise. The mixture was stirred at -78°C for 30 min, at which time additional triethylsilane (9.14 mL, 59.0 mmol) and boron trifluoride etherate (7.97 mL, 62.9 mmol) were added. After the mixture was stirred at -78°C for 2 h, the cooling bath was removed and saturated sodium bicarbonate was added. After 5 min, the mixture was extracted with dichloromethane (3 \times) and the combined organic extracts were dried over sodium sulfate and concentrated in vacuo to give (2S,4R)-di-*tert*-butyl 4-(4-fluorobenzyl)pyrrolidine-1,2-dicarboxylate. This material was dissolved in dichloromethane (50 mL), diluted with trifluoroacetic acid (50 mL), and stirred at room temperature for 5 h. The solution was concentrated in vacuo and dried under high vacuum to give (2S,4R)-4-(4-fluorobenzyl)pyrrolidine-2-carboxylic acid (24.05 g, 90%, trifluoroacetate salt) as a light yellow oil. ^1H NMR (400 MHz, $\text{DMSO}-d_6$): δ 9.98 (br s, 1H), 8.77 (br s, 1H), 7.24 (dd, $J = 8.4, 5.6$ Hz, 2H), 7.10 (t, $J = 8.8$ Hz, 2H), 4.49–4.41 (m, 1H), 3.34–3.24 (m, 1H), 2.91–2.81 (m, 1H), 2.70–2.64 (m, 2H), 2.51–2.42 (m, 1H), 2.11–1.93 (m, 2H). ^{13}C NMR (100 MHz, $\text{DMSO}-d_6$): δ 171.2, 162.8, 160.4, 159.5, 159.2, 136.4, 131.2, 131.1, 115.9, 115.7, 58.9, 50.2, 39.1, 37.0, 33.8. MS (EI) for $\text{C}_{12}\text{H}_{14}\text{FNO}_3$: (224.1, MH^+).

To a solution of the trifluoroacetate salt of (2S,4R)-4-(4-fluorobenzyl)pyrrolidine-2-carboxylic acid (24.05 g, 58.97 mmol) in dioxane (150 mL), acetonitrile (250 mL), and *N,N*-diisopropylethylamine (27.6 mL) at room temperature was added a solution of di-*tert*-butyl

carbonate (18.67 g, 85.70 mmol) in acetonitrile (50 mL). After being stirred at room temperature for 24 h, the mixture was concentrated in vacuo, dissolved in saturated sodium bicarbonate, and washed with ether (3 \times). The aqueous layer was acidified with citric acid to pH 4, then extracted with dichloromethane (3 \times). The combined organic layers were dried over sodium sulfate and concentrated in vacuo to give (2S,4R)-1-(*tert*-butoxycarbonyl)-4-(4-fluorobenzyl)pyrrolidine-2-carboxylic acid (19.02 g, 100% yield) as a yellow oil that solidified on standing. ^1H NMR (400 MHz, $\text{DMSO}-d_6$): δ 12.56 (br s, 1H), 7.23–7.19 (m, 2H), 7.08 (t, $J = 8.6$ Hz, 2H), 4.13–4.09 (m, 1H), 3.37 (dd, $J = 10.2, 7.4$ Hz, 1H), 2.95 (dd, $J = 14.2, 8.2$ Hz, 1H), 2.60 (d, $J = 7.6$ Hz, 2H), 2.44–2.34 (m, 1H), 1.97–1.78 (m, 2H), 1.35 (s, 4H), 1.30 (s, 5H). ^{13}C NMR (100 MHz, $\text{DMSO}-d_6$): δ 174.8, 174.4, 162.6, 160.2, 154.1, 153.7, 137.0, 131.1, 131.0, 115.8, 115.6, 79.4, 79.3, 59.2, 59.0, 51.9, 51.6, 38.6, 37.7, 36.1, 35.4, 28.8, 28.6. MS (EI) for $\text{C}_{17}\text{H}_{22}\text{FNO}_4$: (322.2, MH^+). Mp: 108°C . Anal. Calcd for $\text{C}_{17}\text{H}_{22}\text{FNO}_4$: C, 63.14; H, 6.86; N, 4.33. Found: C, 63.02; H, 7.05; N, 4.26.

A mixture of (2S,4R)-1-(*tert*-butoxycarbonyl)-4-(4-fluorobenzyl)pyrrolidine-2-carboxylic acid (27.50 g, 85.04 mmol), 4-fluorophenoxylaniline (18.15 g, 89.32 mmol), *N,N*-diisopropylethylamine (23 mL), and HATU (34.00 g, 89.42 mmol) in *N,N*-dimethylformamide (80 mL) was stirred at room temperature for 2 h. The mixture was diluted with ethyl acetate, washed with saturated sodium bicarbonate, washed with saturated sodium chloride, dried over sodium sulfate, and concentrated in vacuo. The crude product was purified by flash column chromatography (hexanes/ethyl acetate, 4:1) to give (2S,4R)-*tert*-butyl 4-(4-fluorobenzyl)-2-(4-(4-fluorophenoxy)phenylcarbonyl)pyrrolidine-1-carboxylate (34.50 g, 80% yield) as a yellow oil.

To a solution of (2S,4R)-*tert*-butyl 4-(4-fluorobenzyl)-2-(4-(4-fluorophenoxy)phenylcarbonyl)pyrrolidine-1-carboxylate (34.50 g, 67.84 mmol) in dichloromethane (50 mL) was added trifluoroacetic acid (50 mL) at room temperature. The mixture was stirred at room temperature for 30 min and concentrated in vacuo. The residue was redissolved in dichloromethane (500 mL), washed with saturated sodium bicarbonate, dried over sodium sulfate, and concentrated in vacuo. The residue was triturated with ether (100 mL) and filtered to give **52** (23.65 g, 85% yield) as a colorless solid. ^1H NMR (400 MHz, $\text{DMSO}-d_6$): δ 9.98 (s, 1H), 7.66 (d, $J = 9.2$ Hz, 2H), 7.26–7.18 (m, 4H), 7.10 (t, $J = 8.8$ Hz, 2H), 7.02–6.96 (m, 2H), 6.95 (d, $J = 8.8$ Hz, 2H), 3.77 (dd, $J = 9.2, 4.8$ Hz, 1H), 3.23 (br s, 1H), 2.95 (dd, $J = 10.0, 6.4$ Hz, 1H), 2.63–2.59 (m, 2H), 2.51–2.50 (m, 1H), 2.27–2.16 (m, 1H), 1.91–1.74 (m, 2H). ^{13}C NMR (100 MHz, CDCl_3): δ 173.4, 162.9, 160.4, 160.0, 157.6, 153.7, 153.7, 153.6, 136.3, 136.3, 133.6, 130.2, 130.2, 121.0, 120.1, 120.0, 119.4, 116.6, 116.3, 115.6, 115.3, 60.6, 52.7, 40.7, 38.4, 37.0. MS (EI) for $\text{C}_{24}\text{H}_{22}\text{F}_2\text{N}_2\text{O}_2$: (409.2, MH^+). Mp: 129°C . Anal. Calcd for $\text{C}_{24}\text{H}_{22}\text{F}_2\text{N}_2\text{O}_2$: C, 70.57; H, 5.43; N, 6.86. Found: C, 70.60; H, 5.44; N, 6.83.

A mixture of **52** (23.65 g, 57.90 mmol), 2-(1*H*-1,2,3-triazol-1-yl)acetic acid (7.73 g, 60.8 mmol), *N,N*-diisopropylethylamine (15 mL), and HATU (23.50 g, 61.80 mmol) in *N,N*-dimethylformamide (80 mL) was stirred at room temperature for 1 h. The mixture was diluted with ethyl acetate, washed with saturated sodium bicarbonate, 3 N aqueous hydrochloric acid (2 \times), saturated sodium bicarbonate, and 5% aqueous lithium chloride (2 \times). The organic phase was dried over sodium sulfate and concentrated in vacuo to give a colorless solid. The crude product was treated with a small amount of ethyl acetate and filtered to give **37** (23.87 g, 80% yield) as a colorless solid. ^1H NMR (400 MHz, CDCl_3): δ 8.96 (s, 1H), 7.78 (d, $J = 11.2$ Hz, 2H), 7.43 (d, $J = 9.2$ Hz, 2H), 7.16 (dd, $J = 8.6, 5.0$ Hz, 2H), 7.04–6.98 (m, 4H), 6.94–6.89 (m, 4H), 5.28 (d, $J = 16.0$ Hz, 1H), 5.14 (d, $J = 16.4$ Hz, 1H), 4.80 (d, $J = 7.6$ Hz, 1H), 3.68 (dd, $J = 9.2, 8.0$ Hz, 1H), 3.27 (t, $J = 9.6$ Hz, 1H), 3.02–2.92 (m, 1H), 2.88 (dd, $J = 13.8, 6.6$ Hz, 1H), 2.68 (dd, $J = 14.0, 8.2$ Hz, 1H), 2.61–2.56 (m, 1H), 1.75–1.66 (m, 1H). ^{13}C NMR (100 MHz, CD_3OD): δ 171.0, 165.7, 163.1, 160.6, 160.1, 157.7, 154.2, 153.7, 153.6, 135.9, 135.9, 133.8, 133.2, 130.3, 130.2, 126.5, 121.9, 120.1, 120.0, 118.6, 116.2, 115.9, 115.2, 115.0, 61.1, 51.6, 51.2, 40.1, 37.5, 35.1. IR (KBr pellet): 3285, 2940, 1667, 1605, 1509, 1496, 1209 cm^{-1} . Mp: 170°C . MS (EI) $\text{C}_{28}\text{H}_{25}\text{F}_2\text{N}_5\text{O}_3$: 518.2 (MH^+). High resolution MS: FAB MS using glycerol as matrix.

Calculated for $C_{28}H_{25}F_2N_5O_3$: 518.20039. Found: 518.20038. Optical rotation: $[\alpha]_D -83.7^\circ$ (c 1.0244, EtOH, 25 °C). Anal. Calcd for $C_{28}H_{25}F_2N_5O_3$: C, 64.98; H, 4.87; N, 13.53. Found: C, 64.77; H, 4.80; N, 13.57.

Compounds 31–35 and 38 were prepared according to a similar procedure as described for the synthesis of compound 37.

(2S,4R)-1-(2-(1H-imidazol-5-yl)acetyl)-4-benzyl-N-(4-phenoxyphenyl)pyrrolidine-2-carboxamide (31). 1H NMR (mixture of rotamers, 400 MHz, DMSO- d_6): δ 12.28 (br s, 1H), 10.06 (s, 1H), 7.73–7.75 (m, 3H), 7.33–7.15 (m, 7H), 7.05–6.92 (m, 5H), 4.54–4.48 (m, 1H), 3.76–3.45 (m, 4H), 2.74–2.54 (m, 3H), 1.98–1.87 (m, 2H). MS (EI) for $C_{29}H_{27}FN_4O_3$, found 499.0 (MH^+).

(2S,4S)-1-(2-(1H-imidazol-5-yl)acetyl)-N-(4-phenoxyphenyl)-4-phenylpyrrolidine-2-carboxamide (32). 1H NMR (mixture of rotamers, 400 MHz, DMSO- d_6): δ 11.90 (s, 1H), 10.19 (s, 1H), 7.70–7.58 (m, 3H), 7.39–7.16 (m, 7H), 7.70–6.93 (m, 5H), 4.65–4.58 (m, 1H), 4.09 (t, J = 8.3 Hz, 1H), 3.75–3.44 (m, 4H), 2.41–2.22 (m, 2H). MS (EI) for $C_{28}H_{25}FN_4O_3$, found 484.9 (MH^+).

(2S,4S)-1-(2-(1H-1,2,4-Triazol-1-yl)acetyl)-N-(4-phenoxyphenyl)-4-phenylpyrrolidine-2-carboxamide (33). 1H NMR (400 MHz, $CDCl_3$): δ 9.08 (s, 1H), 8.27 (s, 1H), 8.01 (s, 1H), 7.46 (d, J = 11.8 Hz, 2H), 7.40–7.37 (m, 2H), 7.33–7.29 (m, 3H), 7.04–6.99 (m, 2H), 6.96–6.92 (m, 4H), 5.04 (d, J = 2.9 Hz, 2H), 4.96 (d, J = 7.7 Hz, 1H), 4.06 (t, J = 9.6 Hz, 1H), 3.96–3.86 (m, 1H), 3.61 (t, J = 10.0 Hz, 1H), 2.90 (dd, J = 12.3, 5.9 Hz, 1H), 2.20–2.11 (m, 1H). MS (EI) for $C_{27}H_{24}FN_5O_3$, found 486.2 (MH^+).

(2S,4R)-1-(2-(1H-1,2,4-Triazol-1-yl)acetyl)-4-benzyl-N-(4-phenoxyphenyl)pyrrolidine-2-carboxamide (34). 1H NMR (400 MHz, DMSO- d_6): δ 9.99 (s, 1H), 8.43 (s, 1H), 7.95 (s, 1H), 7.55 (d, J = 9.0 Hz, 2H), 7.36–7.15 (m, 7H), 7.05–6.91 (m, 4H), 5.28 (d, J = 16.9 Hz, 1H), 5.20 (d, J = 16.9 Hz, 1H), 4.54–4.47 (m, 1H), 3.84–3.79 (m, 1H), 3.37–3.33 (m, 1H), 2.78–2.63 (m, 3H), 2.02–1.87 (m, 2H). MS (EI) for $C_{28}H_{26}FN_5O_3$, found 500.0 (MH^+).

(2S,4R)-1-(2-(1H-1,2,4-Triazol-1-yl)acetyl)-4-(4-fluorobenzyl)-N-(4-(4-fluorophenoxy)phenyl)pyrrolidine-2-carboxamide (35). 1H NMR (400 MHz, DMSO- d_6): δ 10.00 (s, 1H), 8.43 (s, 1H), 7.95 (s, 1H), 7.57–7.54 (m, 2H), 7.35–7.08 (m, 6H), 7.05–6.90 (m, 4H), 5.27 (d, J = 16.0 Hz, 1H), 5.18 (d, J = 16.0 Hz, 1H), 4.56–4.47 (m, 1H), 3.87–3.74 (m, 1H), 3.36–3.22 (m, 1H), 2.79–2.62 (m, 3H), 2.04–1.89 (m, 2H). MS (EI) for $C_{28}H_{25}F_3N_5O_3$, found 519.9 (MH^+).

(2S,4R)-1-(2-(2H-1,2,3-Triazol-2-yl)acetyl)-4-(4-fluorobenzyl)-N-(4-(4-fluorophenoxy)phenyl)pyrrolidine-2-carboxamide (38). 1H NMR (400 MHz, DMSO- d_6): δ 9.97 (s, 1H), 8.43 (s, 1H), 7.80 (s, 1H), 7.58–7.51 (m, 2H), 7.34–7.07 (m, 6H), 7.04–6.90 (m, 4H), 5.51 (d, J = 16.7 Hz, 1H), 5.44 (d, J = 16.7 Hz, 1H), 4.53–4.46 (m, 1H), 3.85–3.76 (m, 1H), 3.36–3.32 (m, 1H), 2.77–2.61 (m, 3H), 2.03–1.86 (m, 2H). MS (EI) for $C_{28}H_{25}F_2N_5O_3$, found 519.7 (MH^+).

(2S,4S)-1-(2-(1H-1,2,4-Triazol-1-yl)acetyl)-4-(4-fluorobenzyl)-N-(4-(4-fluorophenoxy)phenyl)pyrrolidine-2-carboxamide (36). A flask was charged with 54 (2.10 g, 9.10 mmol), HATU (3.80 g, 10.0 mmol), 4-(4-fluorophenoxy)aniline (1.85 g, 9.09 mmol), N,N -diisopropylethylamine (4.8 mL, 27 mmol), and DMF (20 mL). The reaction mixture was stirred at room temperature for 30 min, at which time it was quenched with saturated sodium bicarbonate and extracted with ethyl acetate. The organic layer was separated, washed with water, brine, dried over anhydrous sodium sulfate, filtered, and concentrated. The crude mixture was used without further purification.

The crude mixture was combined with HCl (20 mL, 4 N in dioxane) and stirred at room temperature for 1 h, at which time it was quenched with saturated sodium bicarbonate and extracted with ethyl acetate. The organic layer was separated, washed with water, brine, dried over anhydrous sodium sulfate, filtered, and concentrated in vacuo. The crude mixture was triturated with ethyl acetate to provide (2R,4R)-N-(4-(4-fluorophenoxy)phenyl)-4-hydroxypyrrrolidine-2-carboxamide as an off-white solid (1.47 g, 4.65 mmol, 51% yield).

A flask was charged with (2R,4R)-N-(4-(4-fluorophenoxy)phenyl)-4-hydroxypyrrrolidine-2-carboxamide (1.47 g, 4.65 mmol), 2-(1H-1,2,4-triazol-1-yl)acetic acid (591 mg, 4.65 mmol), N,N -diisopropylethylamine (3.0 mL, 17 mmol), HATU (1.90 g, 5.00 mmol), and DMF (10 mL). The reaction mixture was stirred at room temperature for 20 min, at which time it was quenched with saturated sodium bicarbonate

and extracted with ethyl acetate. The organic layer was separated, washed with water, brine, dried over anhydrous sodium sulfate, filtered, and concentrated. The residue was triturated with ethyl acetate to provide 55 as an off-white solid (1.37 g, 3.25 mmol, 70% yield).

To a flask charged with oxalyl chloride (0.165 mL, 1.89 mmol) and DCM (4 mL) at $-78^\circ C$ was added DMSO (3.78 mmol, 0.268 mL) dropwise. The solution was stirred for 15 min before 55 (0.20 g, 0.47 mmol) in DCM (1 mL) was added via syringe. The reaction mixture was then stirred at $0^\circ C$ for 30 min before it was quenched with triethylamine (2.0 mL, 15 mmol). After the mixture was stirred for an additional 5 min, saturated ammonium chloride was added. The organic layer was purified directly by flash chromatography (ethyl acetate to ethyl acetate/methanol (9:1) + 1% NEt_3) to provide the ketone (0.11 g, 0.25 mmol, 53% yield) as a colorless oil.

To a flask charged with NaH (60% dispersion in oil, 124 mg, 3.10 mmol) and DMSO (2 mL) was added 4-fluorobenzyltriphenylphosphine chloride (1.00 g, 2.46 mmol) in DMSO (2 mL). The reaction mixture was stirred at $70^\circ C$ for 3 h, over which time it turned a dark red color. (R)-1-(2-(1H-1,2,4-Triazol-1-yl)acetyl)-N-(4-(4-fluorophenoxy)phenyl)-4-oxopyrrolidine-2-carboxamide (0.11 g, 0.25 mmol) in DMSO (2 mL) was added. The reaction mixture was stirred for 16 h at $70^\circ C$, at which time it was quenched with saturated ammonium chloride and extracted with ethyl acetate. The organic layer was separated, washed with water, and purified directly by flash chromatography (ethyl acetate to ethyl acetate/methanol (9:1) + 1% NEt_3) to provide the alkene (15 mg, 0.027 mmol, 11% yield, mixture of alkene isomers by NMR) as a red oil.

A flask was charged with (R)-1-(2-(1H-1,2,4-triazol-1-yl)acetyl)-4-(4-fluorobenzylidene)-N-(4-(4-fluorophenoxy)phenyl)pyrrolidine-2-carboxamide (15 mg, 0.027 mmol), Pd/C (10%, 50 mg), and methanol (5 mL). The mixture was stirred under a hydrogen atmosphere (balloon) for 2 h at room temperature, at which time it was concentrated and purified by flash chromatography (ethyl acetate to ethyl acetate/methanol (9:1) + 1% NEt_3) to provide 36 (10 mg, 0.019 mmol, 69%) as an off-white solid. 1H NMR (400 MHz, $CDCl_3$): δ 8.61 (s, 1H), 8.22 (s, 1H), 7.98 (s, 1H), 7.45 (d, J = 9.0 Hz, 2H), 7.18–7.14 (m, 2H), 7.03–6.91 (m, 8H), 5.04 (d, J = 16.1 Hz, 1H), 4.95 (d, J = 16.1 Hz, 1H), 4.64–4.60 (m, 1H), 3.76 (dd, J = 10.1, 7.0 Hz, 1H), 3.30–3.20 (m, 1H), 2.85 (dd, J = 13.1, 6.6 Hz, 1H), 2.73 (dd, J = 13.6, 7.9 Hz, 1H), 2.63–2.53 (m, 1H), 2.32–2.28 (m, 2H). MS (EI) for $C_{28}H_{25}F_2N_5O_3$, found 518.2 (MH^+).

(2R,4S)-1-(2-(1H-1,2,3-Triazol-1-yl)acetyl)-4-(4-fluorobenzyl)-N-(4-(4-fluorophenoxy)phenyl)pyrrolidine-2-carboxamide (ent-37). A flask was charged with 56 (5.00 g, 38.8 mmol), *p*-toluenesulfonic acid monohydrate (369 mg, 1.94 mmol), and ethanol (100 mL). The mixture was stirred overnight at room temperature. The reaction mixture was concentrated in vacuo to provide (R)-ethyl 5-oxopyrrolidine-2-carboxylate (38.8 mmol, quant) which was carried forward without further purification.

Conversion of (R)-ethyl 5-oxopyrrolidine-2-carboxylate to ent-37 was done in a similar manner as 37 except the ester hydrolysis was carried out using 2 N KOH/methanol (1:1) in place of trifluoroacetic acid. Upon purification by reverse phase HPLC, ent-37 (115 mg, 23% yield) was provided as an off-white solid. 1H NMR (400 MHz, $CDCl_3$): δ 8.96 (s, 1H), 7.78 (d, J = 11.2 Hz, 2H), 7.43 (d, J = 9.2 Hz, 2H), 7.16 (dd, J = 8.6, 5.0 Hz, 2H), 7.04–6.98 (m, 4H), 6.94–6.89 (m, 4H), 5.28 (d, J = 16.0 Hz, 1H), 5.14 (d, J = 16.4 Hz, 1H), 4.80 (d, J = 7.6 Hz, 1H), 3.68 (dd, J = 9.2, 8.0 Hz, 1H), 3.27 (t, J = 9.6 Hz, 1H), 3.02–2.92 (m, 1H), 2.88 (dd, J = 13.8, 6.6 Hz, 1H), 2.68 (dd, J = 14.0, 8.2 Hz, 1H), 2.61–2.56 (m, 1H), 1.75–1.66 (m, 1H). MS (EI) for $C_{28}H_{25}F_2N_5O_3$, found 518.2 (MH^+).

CNG cAMP Assay. Frozen HEK293 cells expressing the CNG channel and S1P₁ (BD Biosciences, San Jose, CA) were thawed and plated into the wells of a black, clear-bottom, 384-well CellBind plate (Corning, Corning, NY) at 14 000 cells per well. HEK293 cells expressing the CNG channel and CB1 (BD Biosciences) were cultured and plated under the same conditions. The cells were incubated for 16 h at $37^\circ C$ in complete DMEM medium (Invitrogen Carlsbad, CA) containing 10% FBS (HyClone Logan, UT), 250 $\mu g/mL$ Geneticin (Invitrogen), and 1 $\mu g/mL$ puromycin (Sigma-Aldrich, St. Louis, MO). A membrane

potential dye (BD Biosciences) was added, and the plates were incubated for 2–2.5 h at room temperature. Test compounds were tested at maximum concentrations of 10 and 1 μ M for the agonist and antagonist assays, respectively. Compounds were diluted in DMSO (10 concentration points, 3-fold each) and added to the assay plate at a final DMSO concentration of 0.5%. For each compound, there were duplicate assay plates and each assay plate had duplicate wells per concentration point. Test compounds were added to the cells in a DPBS solution containing 25 μ M Ro 20-1724 (Sigma-Aldrich), 500 nM A2b receptor agonist NECA (Sigma-Aldrich), and 10 nM (EC₉₅) Merck S1P₁ agonist (**26**) or S1P (Avanti Alabaster, AL) and incubated for 90 min. For CB1, the competing agonist was 10 nM CP-55940 (Sigma-Aldrich). The assay plate was read before compound addition (T_0) and after the 90 min incubation (T_{90}) using an EnVision plate reader (PerkinElmer, Waltham, MA) at an excitation wavelength of 350 nm and an emission wavelength of 590 nm. The T_{90}/T_0 ratio was determined for each concentration of the test compounds. The percent antagonist activity was determined as $[(\text{test compound} - \text{agonist alone control}) / (\text{NECA alone control} - \text{agonist alone control})] \times 100$. The percent activities were plotted against compound concentration to determine IC₅₀ using XLFit (IDBS, Alameda, CA).

Luciferase Selectivity Assay. For the Tango β -arrestin recruitment assay (luciferase selectivity assay), the cytoplasmic C-terminus of S1P₁ is tethered to the tTA transcriptional activator with a linker that contains a cleavage site for the N1a protease from tobacco etch virus (TEV protease). The C-terminus of the human β -arrestin 2 protein is fused to TEV protease. Binding of an agonist recruits the β -arrestin-TEV fusion protein to the receptor, resulting in cleavage of the linker and release of tTA to enter the nucleus and subsequently activate a tTA-dependent luciferase reporter gene. Frozen HEK293 cells transiently transfected with receptor cDNAs for S1P₁, S1P₂, or S1P₃ (Invitrogen) were thawed and suspended in 10 mL of Pro293a-CDM culture medium (Invitrogen) supplemented with 4 mM L-glutamine (Invitrogen), 1 \times Pen/Strep (100 units/mL penicillin and 100 μ g/mL streptomycin, Invitrogen), and 0.1% fatty acid free BSA (Sigma-Aldrich). Cells were added to the wells of a 384-well white opaque bottom assay plate (PerkinElmer) at 3000–6000 cells per well, and the plate was incubated for approximately 4 h in a 37 °C incubator. Test compounds were tested at maximum concentrations of 1 μ M. Compounds were diluted in DMSO (10 concentration points, 3-fold each) and added to the assay plate at a 1% final DMSO concentration. For each compound, there were duplicate assay plates and each assay plate had duplicate wells per concentration point. The plate was incubated at 37 °C for 30 min. For S1P₁, S1P₂, and S1P₃ antagonist assays, the agonist S1P was added at a final EC₉₅ concentration of 400, 100, and 400 nM, respectively. Following agonist additions, the assay plates were incubated in a 37 °C incubator for 16–18 h. Luciferase assay reagent was added and luminescence measured in an EnVision plate reader (PerkinElmer). Percent antagonist activity was determined as $[(\text{positive control} - \text{test compound}) / (\text{positive control} - \text{background})] \times 100$, where background is the luminescence of the DMSO control and the positive control is the luminescence from cells incubated with 400 nM (EC₉₅) S1P. The percent activities were plotted against compound concentration to determine IC₅₀ using XLFit (IDBS).

■ ASSOCIATED CONTENT

■ Supporting Information

Materials and methods used in determination of pharmacokinetic, efficacy, MLM oxidation, and CYP450 inhibition data. This material is available free of charge via the Internet at <http://pubs.acs.org>.

■ AUTHOR INFORMATION

Corresponding Author

*Phone: (650) 837-7006. Fax: (650) 837-8177. E-mail: hjohnson@exelixis.com.

■ ACKNOWLEDGMENTS

The authors thank Siamak Dailami for analytical support; Lory Tan and John Bui for collecting the reported ADME data; Atulkumar Ramaiya, Ron Aoyama, Scott Womble, and Michael Yakes for obtaining PK data; Eliana Bustamante, Dorothy Trent, Melanie Dimapasoc, Yelena Zhrebina, Shaun Nguyen, and Josh Rulloda in Compound Repository; Fawn Qian and Danny Tam from Molecular and Cellular Pharmacology; and Amy Lew for editorial comments.

■ ABBREVIATIONS USED

S1P, sphingosine 1-phosphate; S1P₁, sphingosine 1-phosphate receptor 1; MLM, mouse liver microsome; HATU, O-(7-azabenzotriazol-1-yl)-N,N,N',N'-tetramethyluronium hexafluorophosphate; CBz, benzyl carbamate

■ REFERENCES

- (1) Zhang, H.; Desai, N. N.; Olivera, A.; Seki, T.; Brooker, G.; Spiegel, S. Sphingosine-1-phosphate, a novel lipid, involved in cellular proliferation. *J. Cell Biol.* **1991**, *114*, 155–167.
- (2) Cuvillier, O.; Pirianov, G.; Kleuser, B.; Vanek, P. G.; Coso, O. A.; Gutkind, J. S.; Spiegel, S. Suppression of ceramide-mediated programmed cell death by sphingosine-1-phosphate. *Nature* **1996**, *381*, 800–803.
- (3) Wang, F.; Van Brocklyn, J. R.; Hobson, J. P.; Movafagh, S.; Zukowska-Grojec, Z.; Milstien, S.; Spiegel, S. Sphingosine 1-phosphate stimulates cell migration through a G_i-coupled cell surface receptor: potential involvement in angiogenesis. *J. Biol. Chem.* **1999**, *274*, 35343–35350.
- (4) Lee, M.-J.; Thangada, S.; Claffey, K. P.; Ancellin, N.; Liu, C. H.; Kluk, M.; Volpi, M.; Sha'afi, R. I.; Hla, T. Vascular endothelial cell adherens junction assembly and morphogenesis induced by sphingosine-1-phosphate. *Cell* **1999**, *99*, 301–312.
- (5) Graeler, M.; Shankar, G.; Goetzl, E. J. Cutting edge: suppression of T cell chemotaxis by sphingosine 1-phosphate. *J. Immunol.* **2002**, *169*, 4084–4087.
- (6) Lee, M.-J.; Van Brocklyn, J. R.; Thangada, S.; Liu, C. H.; Hand, A. R.; Menzeleev, R.; Spiegel, S.; Hla, T. Sphingosine-1-phosphate as a ligand for the G protein-coupled receptor EDG-1. *Science* **1998**, *279*, 1552–1555.
- (7) Hla, T.; Maciag, T. An abundant transcript induced in differentiating human endothelial cells encodes a polypeptide with structural similarities to G-protein-coupled receptors. *J. Biol. Chem.* **1990**, *265*, 9308–9313.
- (8) Liu, Y.; Wada, R.; Yamashita, T.; Mi, Y.; Deng, C. X.; Hobson, J. P.; Rosenfeldt, H. M.; Nava, V. E.; Chae, S. S.; Lee, M. J.; Liu, C. H.; Hla, T.; Spiegel, S.; Proia, R. L. Edg-1, the G protein-coupled receptor for sphingosine-1-phosphate, is essential for vascular maturation. *J. Clin. Invest.* **2000**, *106*, 951–961.
- (9) Brinkmann, V.; Billich, A.; Baumruker, T.; Heining, P.; Schmouder, R.; Francis, G.; Aradhye, S.; Burtin, P. Fingolimod (FTY720): discovery and development of an oral drug to treat multiple sclerosis. *Nat. Rev. Drug Discovery* **2010**, *9*, 883–897.
- (10) Marsolais, D.; Rosen, H. Chemical modulators of sphingosine-1-phosphate receptors as barrier-oriented therapeutic molecules. *Nat. Rev. Drug Discovery* **2009**, *8*, 297–307.
- (11) Buzard, D. J.; Thatte, J.; Lerner, M.; Edwards, J.; Jones, R. M. Recent progress in the development of selective S1P1 receptor agonists for the treatment of inflammatory and autoimmune disorders. *Expert Opin. Ther. Pat.* **2008**, *18*, 1141–1159.
- (12) Yonesu, K.; Nakamura, T.; Mizuno, Y.; Suzuki, C.; Nagayama, T.; Satoh, S.; Nara, F. A novel sphingosine-1-phosphate receptor 1 antagonist prevents the proliferation and relaxation of vascular endothelial cells by sphingosine-1-phosphate. *Biol. Pharm. Bull.* **2010**, *33*, 1500–1505.
- (13) Nakamura, T.; Yonesu, K.; Mizuno, Y.; Suzuki, C.; Sakata, Y.; Takuwa, Y.; Nara, F.; Satoh, S. Synthesis and SAR studies of a novel

class of S1P₁ receptor antagonists. *Bioorg. Med. Chem.* **2007**, *15*, 3548–3564.

(14) Sanna, M. G.; Wang, S. K.; Gonzalez-Cabrera, P. J.; Don, A.; Marsolais, D.; Matheu, M. P.; Wei, S. H.; Parker, I.; Jo, E.; Cheng, W.; Cahalan, M. D.; Wong, C.-H.; Rosen, H. Enhancement of capillary leakage and restoration of lymphocyte egress by a chiral S1P₁ antagonist in vivo. *Nat. Chem. Biol.* **2006**, *2*, 434–441.

(15) Inoki, I.; Takuwa, N.; Sugimoto, N.; Yoshioka, K.; Takata, S.; Kaneko, S.; Takuwa, Y. Negative regulation of endothelial morphogenesis and angiogenesis by S1P₂ receptor. *Biochem. Biophys. Res. Commun.* **2006**, *346*, 293–300.

(16) Sanna, M. G.; Liao, J.; Euijung, J.; Alfonso, C.; Anh, M.-Y.; Peterson, M. S.; Webb, B.; Lefebvre, S.; Chun, J.; Gray, N.; Rosen, H. Sphingosine 1-phosphate (S1P) receptor subtypes S1P₁ and S1P₃, respectively, regulate lymphocyte recirculation and heart rate. *J. Biol. Chem.* **2004**, *279*, 13839–13848.

(17) Ryan, A. J.; Wedge, S. R. ZD6474—a novel inhibitor of VEGFR and EGFR tyrosine kinase activity. *Br. J. Cancer.* **2005**, *92*, S6–S13.

(18) Hale, J. J.; Lynch, C. L.; Neway, W.; Mills, S. G.; Hajdu, R.; Keohane, C.; Rosenbach, M. J.; Milligan, J. A.; Shei, G.-J.; Parent, S. A.; Chrebet, G.; Bergstrom, J.; Card, D.; Ferrer, M.; Hodder, P.; Strulovici, B.; Rosen, H.; Mandala, S. A rational utilization of high-throughput screening affords selective, orally bioavailable 1-benzyl-3-carboxyazetidide sphingosine-1-phosphate-1 receptor agonists. *J. Med. Chem.* **2004**, *47*, 6662–6665.

(19) Veber, D. F.; Johnson, S. R.; Cheng, Y.-H.; Smith, B. R.; Ward, K. W.; Kopple, K. D. Molecular properties that influence the oral bioavailability of drug candidates. *J. Med. Chem.* **2002**, *45*, 2615–2623.

(20) Ibrahim, M. A.; Jeong, J. W.; Johnson, H. W. B.; Kearney, P.; Leahy, J. W.; Lewis, G. L.; Noguchi, R. T.; Nuss, J. M. Sphingosine-1-Phosphate Receptor Antagonists. PCT Int. Appl. WO201045580A1, 2010.

(21) Baldwin, J. E.; Miranda, T.; Maloney, M. Amino acid synthesis using (L)-pyroglutamic acid as a chiral starting material. *Tetrahedron* **1989**, *45*, 7459–7468.

(22) Ganellin, C. R.; Bishop, P. B.; Bambal, R. B.; Chan, S. M. T.; Leblond, B.; Moore, A. N. J.; Zhao, L.; Bourgeat, P.; Rose, C.; Vargas, F.; Schwartz, J.-C. Inhibitors of tripeptidyl peptidase II. 3. Derivation of butabindide by successive structure optimizations leading to a potential general approach to designing exopeptidase inhibitors. *J. Med. Chem.* **2005**, *48*, 7333–7342.